Heavy Flavor Kinematic Correlations in Cold and Hot Nuclear Matter

R. Vogt

Lawrence Livermore National Laboratory, Livermore, CA 94551, USA
Physics Department, University of California, Davis, CA 95616, USA

based on:
RV, Phys. Rev. C 98 (2018) 034907
RV, Phys. Rev. C 101 (2020) 024910

Figure 1: This work was performed under the auspices of the U.S. Department of Energy by Lawrence Livermore National Laboratory under Contract DE-AC52-07NA27344 and supported by the U.S. Department of Energy, Office of Science, Office of Nuclear Physics (Nuclear Theory) under contract number DE-SC-0004014.

Outline

- **Motivation for kinematic correlation studies**
- **Heavy flavor production models**
  - **Fragmentation**
  - **k_T broadening**
  - **Comparison to single inclusive p_T data**
- **Heavy flavor pairs**
  - **Effects of fragmentation and broadening on pair production**
  - **$c\bar{c}$ comparison with collider data**
  - **$b\bar{b} \rightarrow J/\psi J/\psi$ comparison with data**
- **Nuclear matter effects on single distributions and pairs**

Motivation I

- **Single inclusive measurements provide some information but, especially in the case of nucleus-nucleus collisions, there are many models**
- **In-medium models have trouble describing both low and high p_T simultaneously**

Many Different Models Try to Describe $A + A$ Collisions

Several collaborative projects made model comparisons to study similarities and differences, see arXiv:1803.03024 [hep-ph] and arXiv:1809.07894 [hep-ph]

Models involve different approaches to:

- **Initial heavy flavor distributions and cold nuclear matter effects**
- **Heavy quark hadronization**
- **Heavy flavor transport**
- **Bulk evolution of the system**

For the initial state, several models use distributions from FONLL (or ZM-VFN scheme – SCET only); others use power-law fits to these distributions, leading order calculations – with supplements, or the PYTHIA event generator (default or tuned to match pQCD results)

Some include shadowing but many do not (if not included in the initial calculations, it is basically impossible to know appropriate inputs to add on later)

Hadronization models sometimes depend on the bulk evolution, other times not. Some approaches use the FONLL fragmentation functions, others use the Peterson fragmentation function (default or tuned). Some use these hard, pp-inspired fragmentation functions together with in-medium appropriate hadronization mechanisms such as regeneration/coalescence/recombination

Difficult for Models to Explain Both R_{AA} and v_2

At low p_T, the results reflect collective motion of the system, possible thermalization; at higher p_T, heavy hadrons spend less time in the medium, more susceptible to energy loss

R_{AA} is the nuclear modification factor, ratio per nucleon of cross section in $A+A$ collisions relative to $p+p$ collisions at the same energy

Elliptic flow, v_2, related to initial spatial anisotropy of the system, azimuthal momentum-space anisotropy of particle emission

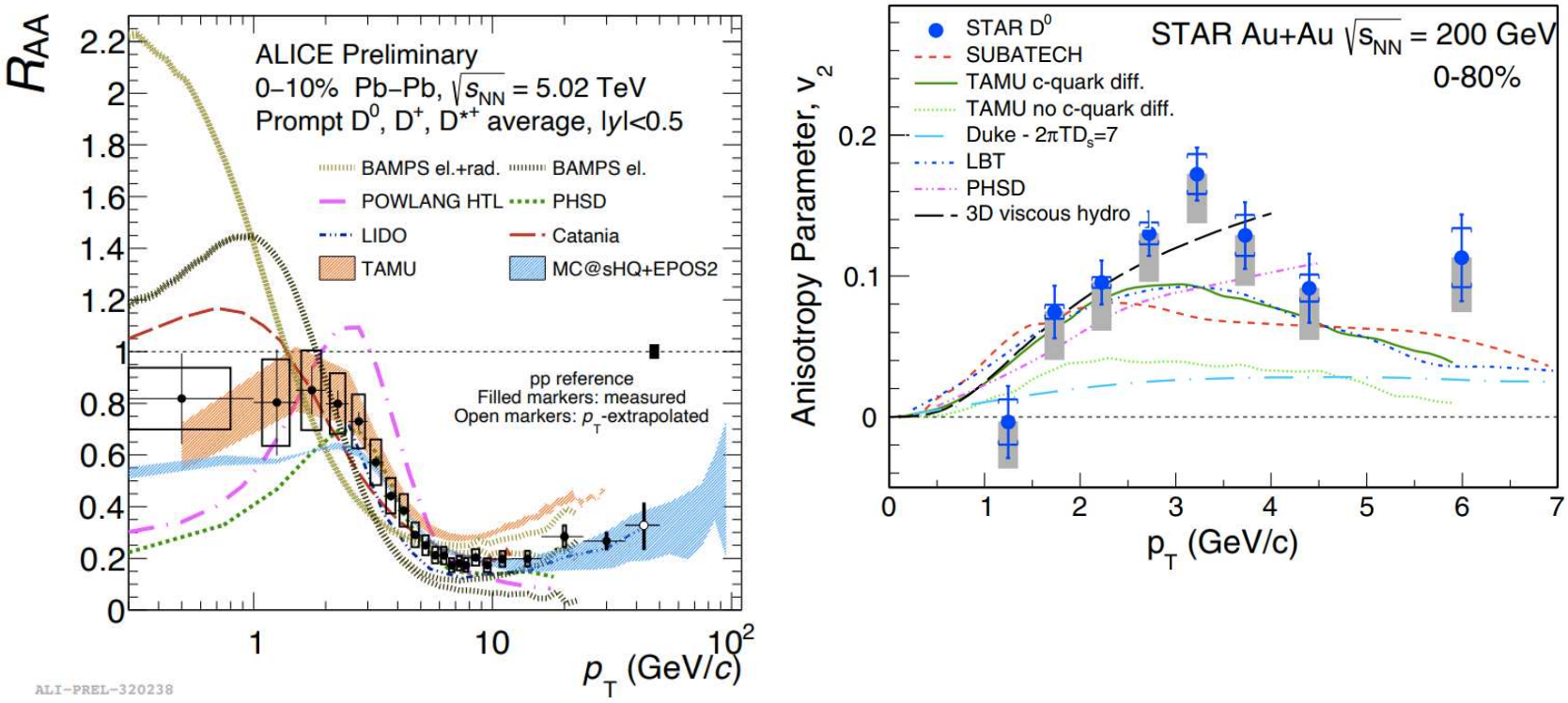

Figure 2: (Left) ALI-PREL-320238 (Right) STAR Collaboration, PRL **118**, 212301 (2017).

Mass Matters: clear hierarchy of suppression in $A + A$ based on quark mass: Dead Cone Effect

Light hadrons most strongly suppressed, charm less suppressed at low p_T than light hadrons, the R_{AA} becomes similar at $p_T \gg m_c$, same trend seen for bottom hadrons but at higher p_T

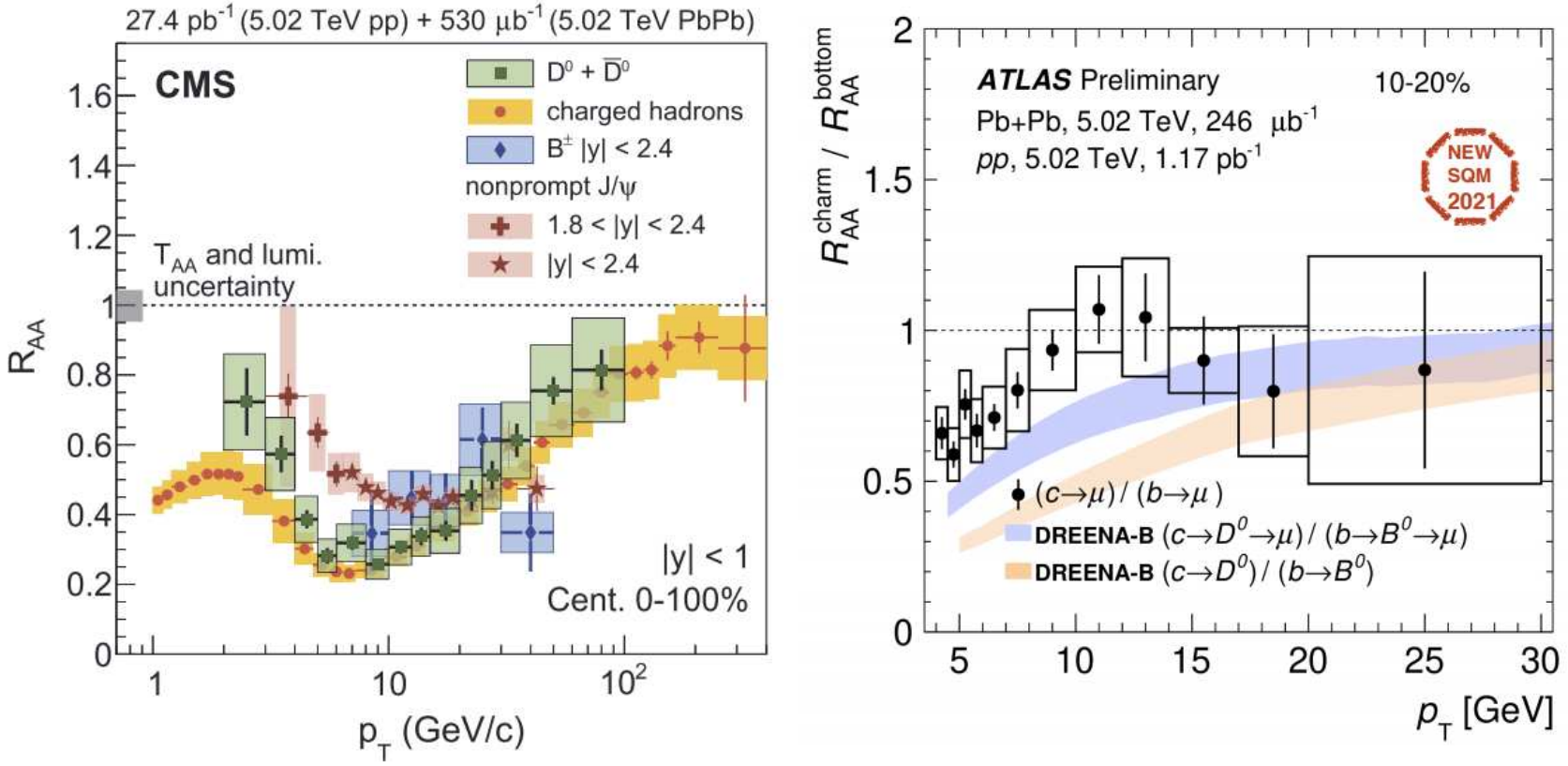

Figure 3: (Left) CMS, Phys. Lett. B **782** (2018) 474. (Right) ATLAS Collaboration, first shown at Strangeness in Quark Matter 2021.

Motivation II

- **Go back to more elementary collisions, $p+p$ and $p+A$**
- **Correlations are more complex observables of heavy flavor production**
- **Naive expectation is that pairs are produced back-to-back (as at leading order) but next-to-leading order contributions change correlation**

Production and Decay of $Q\overline{Q}$ Pairs

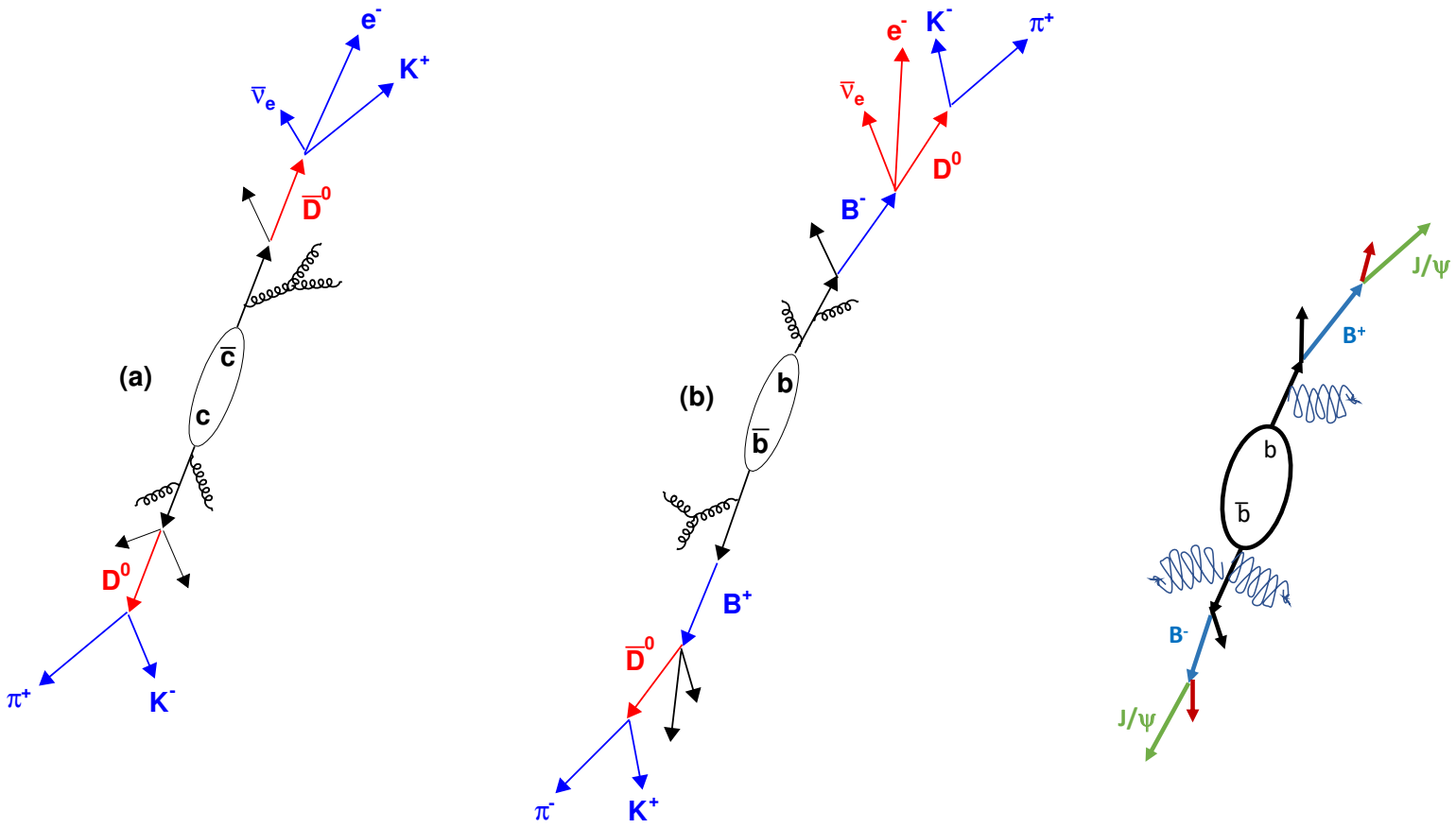

Figure 4: Production and decay of $c\overline{c}$ and $b\overline{b}$ pairs to hadrons. (Figures (a) and (b) courtesy of Andre Mischke.)

Contributions to $Q\overline{Q}$ Pair Production

Only gg and $q\overline{q}$ at LO, at NLO there is new channel, $q(\overline{q})g$

Contributions sorted by initial state, not diagram topology as in LO event generators with labels like flavor creation, flavor excitation and gluon splitting

These labels are for topologies, not production mechanisms, and are properly weighted in a NLO calculation by color factors, then initial state contributions are summed and amplitudes squared, not possible in event generators

Squaring amplitudes of individual diagrams, as in LO generators, eliminates interferences and will not produce correct cross sections

Some experiments use LO event generators and try to model data by fitting individual diagram weights, this is not really how QCD works

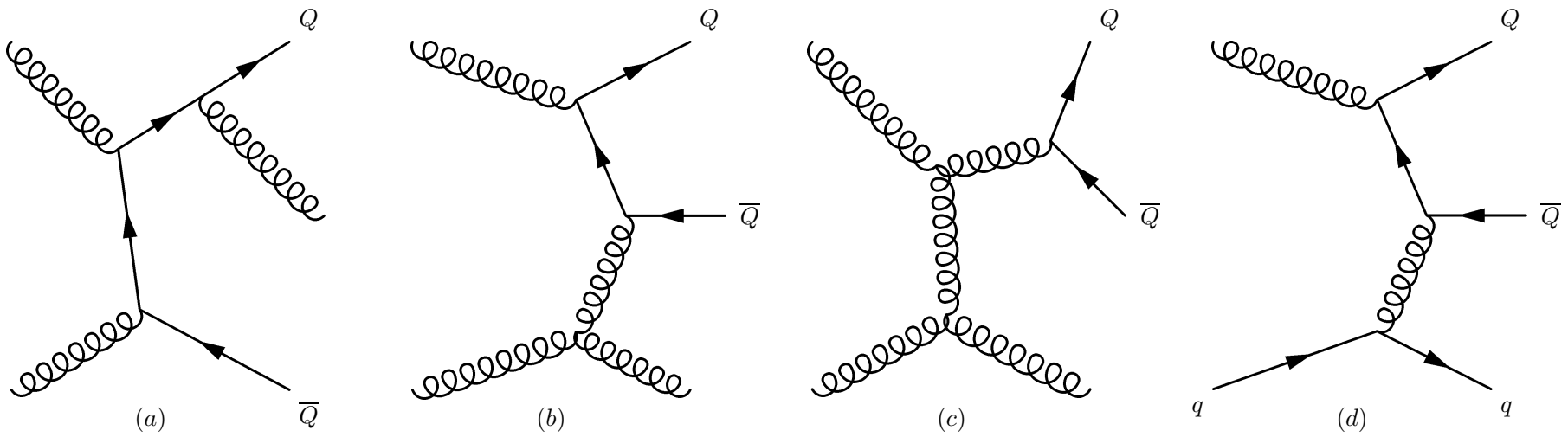

Figure 5: Examples of real contributions to next-to-leading order $Q\overline{Q}$ production. Diagrams (a)-(c) illustrate contributions to $gg \to Q\overline{Q}g$ while (d) shows an example of $qg \to qQ\overline{Q}$ production.

Calculating Heavy Flavors in Perturbative QCD

Hard processes have a large scale in the calculation that makes perturbative QCD applicable, since $m \neq 0$, heavy quark production is a hard process

Total cross section **in a pp collision, assuming collinear factorization**

$$\sigma_{pp}(s, m^2) \;=\; \sum_{i,j=q,\overline{q},g} \int_{4m_Q^2/s}^1 \frac{d\tau}{\tau} \int dx_1\, dx_2\, \delta(x_1 x_2 - \tau) f_i^p(x_1, \mu_F^2)\, f_j^p(x_2, \mu_F^2)\, \widehat{\sigma}_{ij}(\hat{s}, m^2, \mu_F^2, \mu_R^2)$$

f_i^A are nonperturbative parton distributions, determined from global analyses of data sets over many scales, x_1, x_2 are proton momentum fractions carried by partons i and j, $\tau = \hat{s}/s$

$\widehat{\sigma}_{ij}(\hat{s}, m^2, \mu_F^2, \mu_R^2)$ is hard partonic cross section calculable in QCD in powers of α_s^{2+n}: leading order (LO), $n = 0$; next-to-leading order (NLO), $n = 1$ ...

Schematic *single inclusive* heavy flavor production

$$E\frac{d^3\sigma_{\rm fs}}{d^3p} = E_Q \frac{d^3\sigma_Q}{d^3p_Q} \otimes D(Q \to H_Q) \otimes f(H_Q \to {\rm fs})$$

Results depend strongly on quark mass, m, factorization scale, μ_F, in the parton densities and renormalization scale, μ_R, in α_s

FONLL and ZM-VFN schemes treat heavy quark as light for large p_T/m logs at high p_T, match massive and massless parts

Calculating Theoretical Uncertainties

Scales fit to total heavy flavor cross section data

- **Take lattice value for m_c and $1S$ value for m_b, 1.27 ± 0.09 and 4.65 ± 0.09 GeV respectively**
- **Vary scales independently within 1σ of fitted region:**
  $(\mu_F/m, \mu_R/m) =$ **(C,C), (H,H), (L,L), (H,C), (C,H), (L,C), (C,L)**
- **For charm production, $(mu_F/m_T, \mu_R/m_T) = (2.1^{+2.55}_{-0.85}, 1.6^{+0.11}_{-0.12})$ while for bottom production, $(\mu_F/m_T, \mu_R/m_T) = (1.4^{+0.77}_{-0.49}, 1.1^{+0.22}_{-0.20})$**

The uncertainty band in all cases comes from the upper and lower limits of mass and scale uncertainties added in quadrature

$$\frac{d\sigma_{\rm max}}{dX} = \frac{d\sigma_{\rm cent}}{dX} + \sqrt{\left(\frac{d\sigma_{\mu,\rm max}}{dX} - \frac{d\sigma_{\rm cent}}{dX}\right)^2 + \left(\frac{d\sigma_{m,\rm max}}{dX} - \frac{d\sigma_{\rm cent}}{dX}\right)^2},$$

$$\frac{d\sigma_{\rm min}}{dX} = \frac{d\sigma_{\rm cent}}{dX} - \sqrt{\left(\frac{d\sigma_{\mu,\rm min}}{dX} - \frac{d\sigma_{\rm cent}}{dX}\right)^2 + \left(\frac{d\sigma_{m,\rm min}}{dX} - \frac{d\sigma_{\rm cent}}{dX}\right)^2},$$

The resulting theoretical uncertainties can be large, especially for charm

Examples of Total Cross Section Calculations

Fitting the scale factors to the total cross section reduces uncertainties

Charm total cross section fits only done to RHIC energy but agrees with published LHC data

Bottom total cross section measurements show more fluctuations but tighter fit

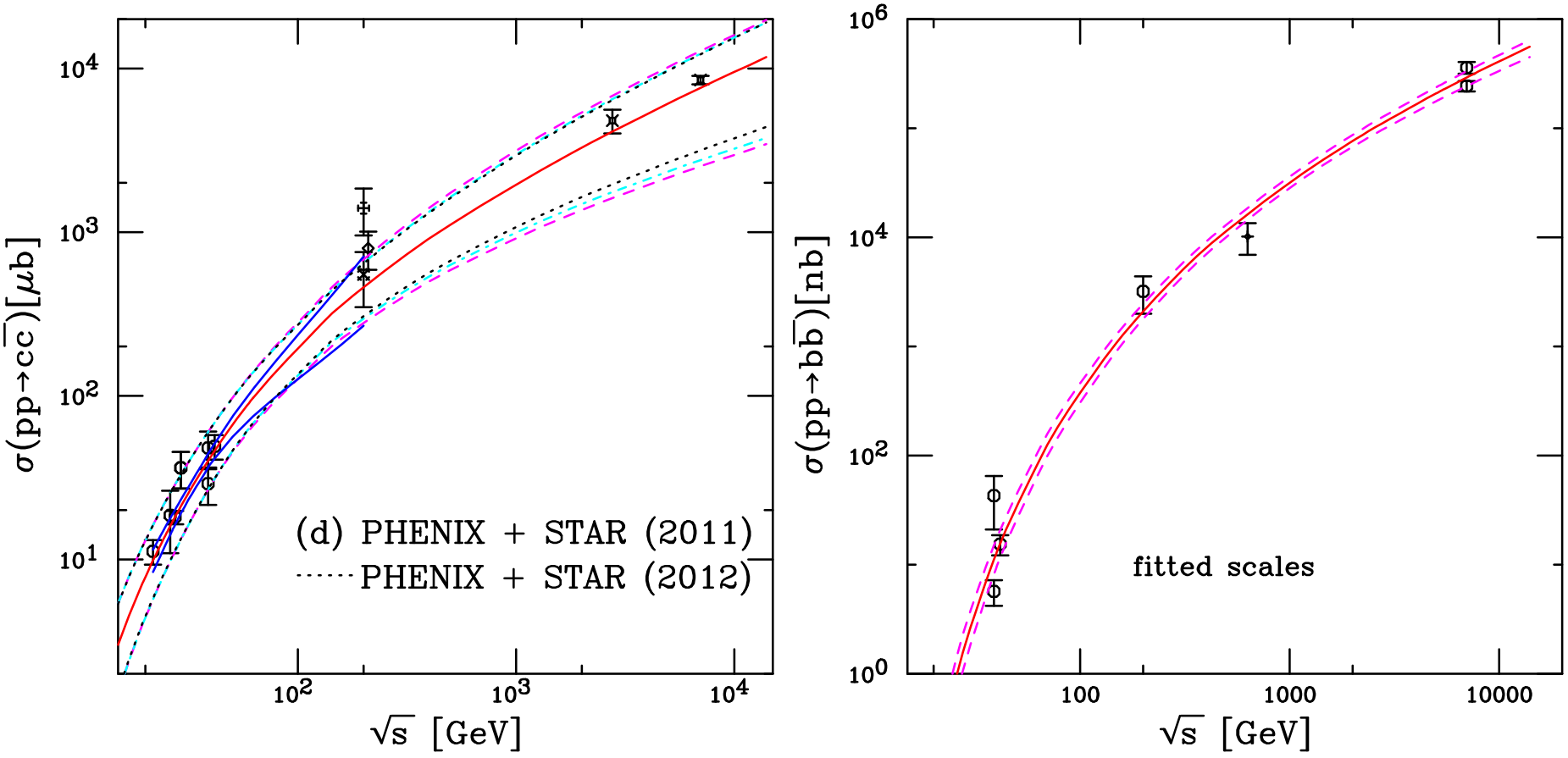

Figure 6: **(Left)** $c\bar{c}$**, (Right)** $b\bar{b}$**, Nelson, Frawley and RV**

Examples of Single Inclusive Calculations

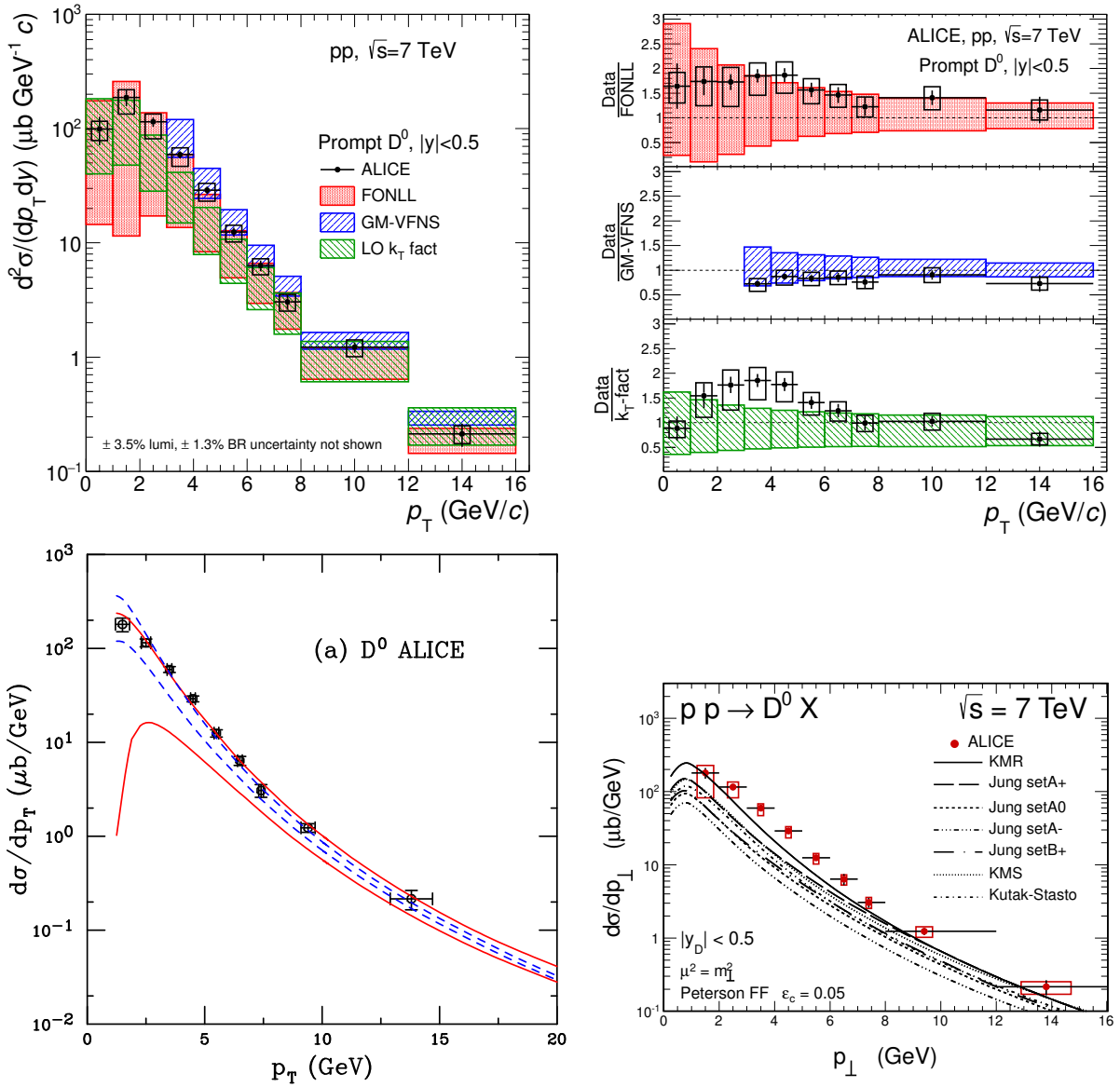

Figure 7: **(Top) ALICE Collaboration, Phys. Rev. C 94 (2016) 05490. (Bottom left) Nelson, Frawley and RV (Bottom right) Maciula and Szczurek**

Production of *Correlated* $Q\overline{Q}$ Pairs

Different levels of exclusivity in heavy flavor production:

- **Total cross sections (all momenta integrated away)**
- **Single inclusive (keeps only momentum of one quark or antiquark, momenta of other final-state partons integrated away)**
- **Exclusive pair production (Keeps momenta of all final-state partons)**

Exclusive calculations needed for correlations, retains all kinematic quantities

Two general approaches:

- **HVQMNR (Mangano, Nason and Ridolfi): no resummation, negative weight MC, incomplete numerical cancellation of divergences at $p_T \to 0$, Peterson function is default fragmentation scheme**
- **POWHEG-hvq (Frixione, Nason and Ridolfi): leading log resummation, positive weight MC, generally interfaces with parton shower LO MC like HERWIG or PYTHIA for fragmentation and decay**

In this work, HVQMNR is used to calculate correlations with fragmentation function and k_T broadening adjusted to reproduce FONLL p_T distribution with same m_Q, μ_F and μ_R

Implementing Fragmentation

FONLL uses different fragmentation schemes for charm and bottom

charm quarks: Calculation based on Mellin moments compared to e^+e^- data; combination of pseudoscalar and vector fragmentation for ground state and excited D mesons, respectively, $\langle z \rangle = 0.822$ for sum of two

bottom quarks: Polynomial

$$D(z) = z(1-z)^{\epsilon}$$

$\epsilon = 27.5$ **for** $m_b = 4.65$ **GeV,** $\langle z \rangle = 0.934$

HVQMNR employs Peterson function for fragmentation with parameter ϵ_P for both charm and bottom,

$$D(z) = \frac{z(1-z)^2}{((1-z)^2 + z\epsilon_P)^2}$$

- **Standard values of ϵ_P, 0.06 for charm and 0.006 for bottom are too large for hadroproduction, $\langle z \rangle = 0.67$ for c and 0.82 for b**
- **To match the FONLL result at high p_T, with k_T broadening, ϵ_P needs to be reduced to 0.008 and 0.0004 for c and b respectively, resulting in $\langle z \rangle = 0.822$ and 0.930 for c and b**

Adjustment of HVQMNR Fragmentation Functions

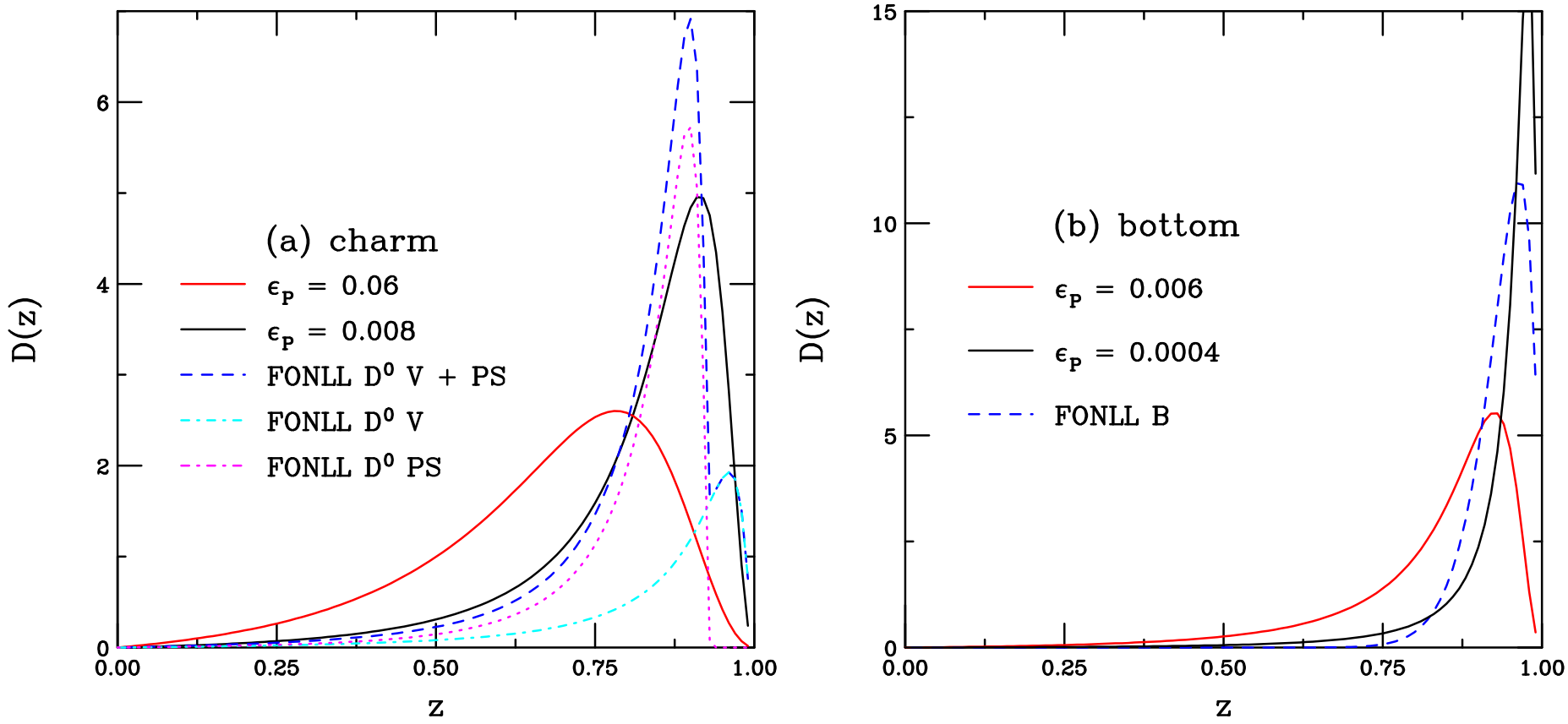

Figure 8: **The fragmentation functions used in the HVQMNR code and FONLL for (a) charm and (b) bottom are compared. The red curves show the standard Peterson function parameter while the black curves are calculated with the values of ϵ_P used in this paper. The FONLL results are shown in the dashed blue curves. For charm quarks, the total FONLL contribution to D^0 fragmentation includes the vector (V) and pseudoscalar (PS) contributions, shown separately.**

Implementation of k_T Broadening

FONLL only includes fragmentation, not broadening

Default HVQMNR combines broadening with fragmentation based on p_T distributions at fixed-target energies: including standard Peterson ϵ_P reduced average p_T at fixed-target energies considerably; rather large k_T broadening had to be included to make up difference and match data

Precedent from Drell-Yan, k_T broadening included to make low p_T distribution finite and take the place of full resummation

$$g(k_T) = \frac{1}{\pi \langle k_T^2 \rangle} \exp(-k_T^2/\langle k_T^2 \rangle)$$

In HVQMNR Gaussian factors are applied to each heavy quark in the final state, should be equivalent to application to initial-state partons as long as $\langle k_T^2 \rangle \sim 2 - 3$ GeV^2

Energy dependence of broadening assumed,

$$k_T^2 = 1 + \frac{1}{n} \ln \left(\frac{\sqrt{s}}{20\,\mathrm{GeV}} \right) \ \mathrm{GeV}^2$$

n fixed from J/ψ and Υ p_T distributions, $n = 12$ for c and 3 for b

Fragmentation and Broadening on Single Inclusive p_T Distributions

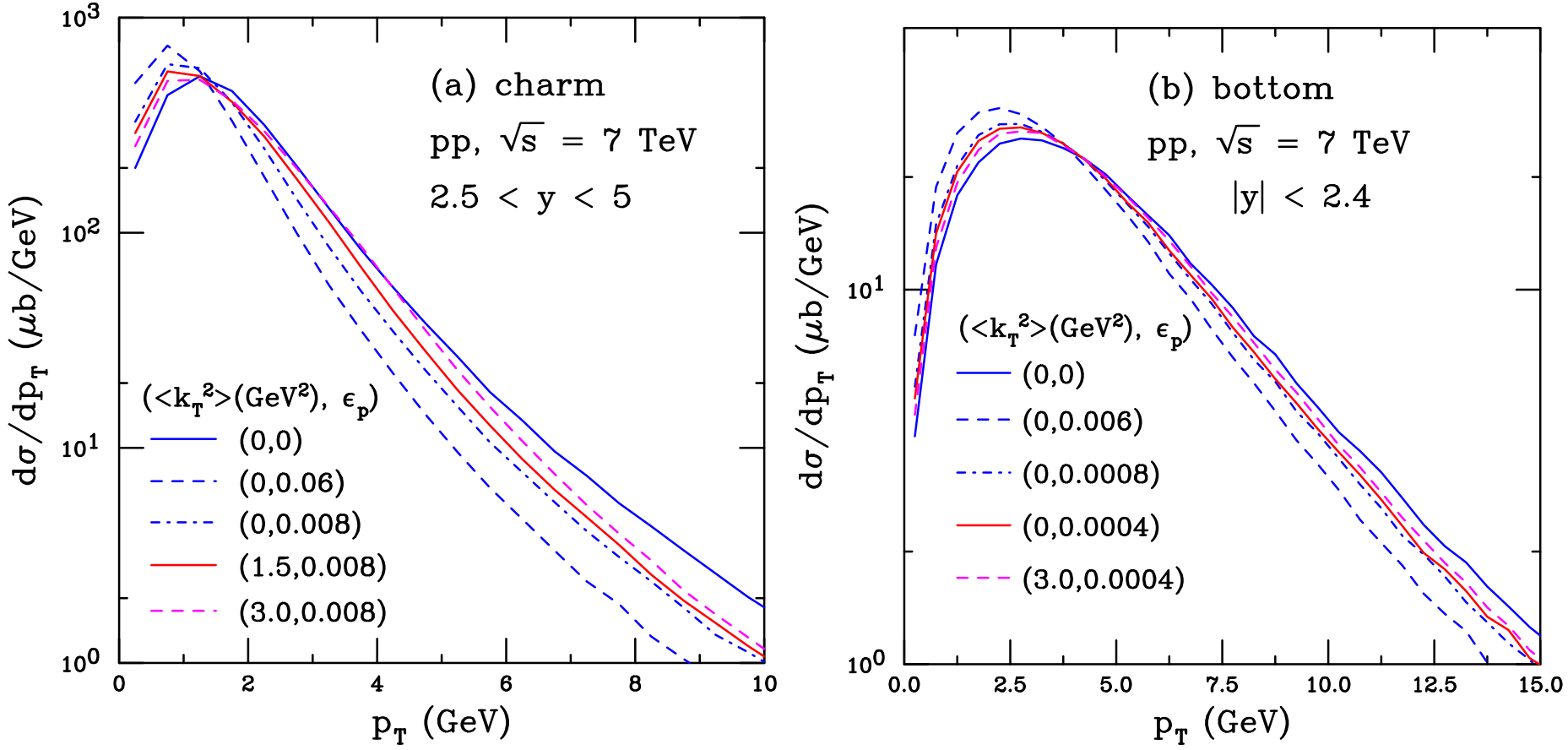

Figure 9: **The single inclusive (a) charm and (b) bottom quark distributions in $\sqrt{s} = 7$ TeV $p + p$ collisions at next-to-leading order using the HVQMNR code. The charm distributions are given at forward rapidity, $2.5 < y < 5$, while the bottom quark distributions are given at midrapidity, $|y| < 2.4$. Results are shown for various combinations of $\langle k_T^2 \rangle$ and ϵ_P.**

Single Hadron p_T Distributions: FONLL and HVQMNR

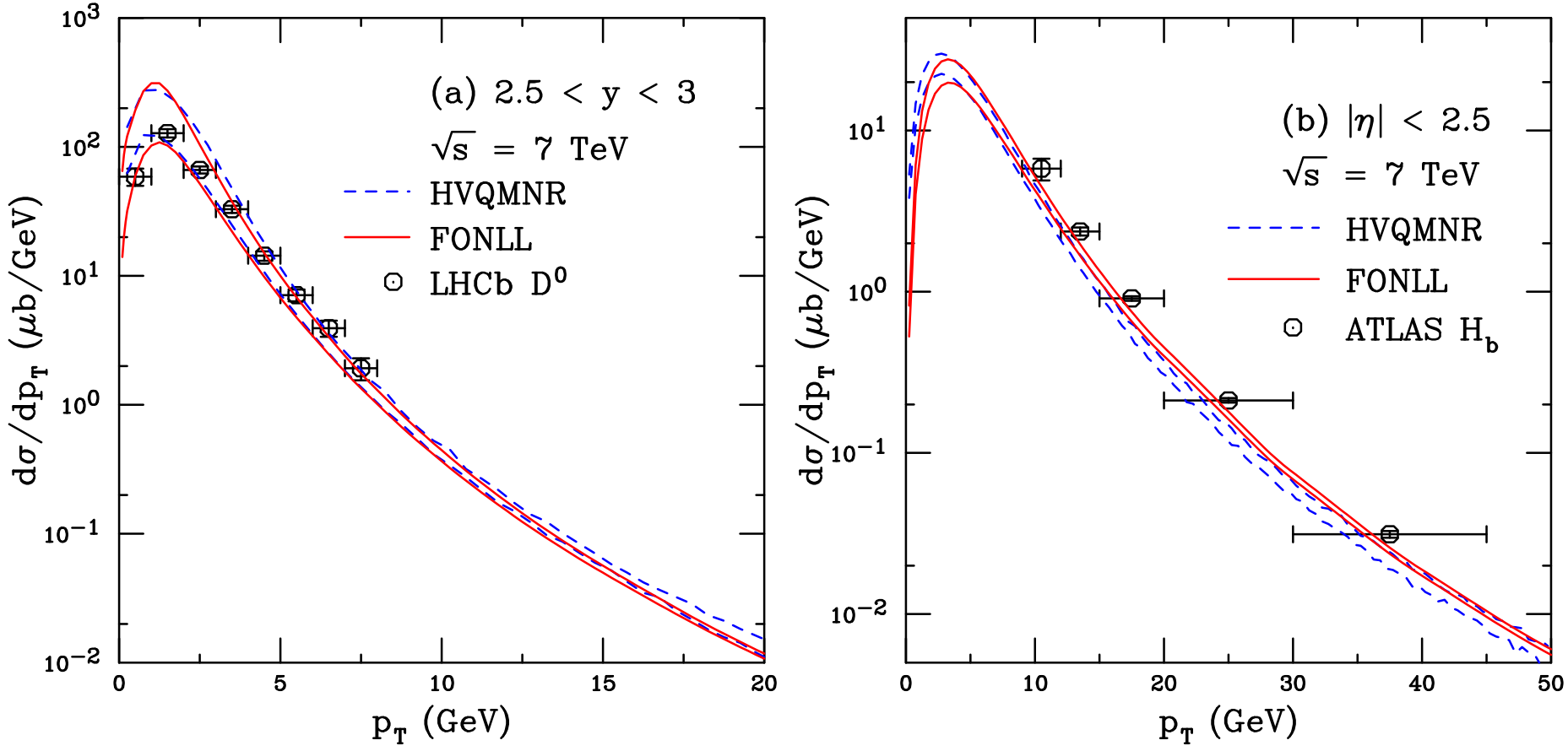

Figure 10: **The single inclusive (a) D^0 and (b) b-quark hadron, H_b, distributions in $\sqrt{s} = 7$ TeV $p + p$ collisions are compared to data from LHCb (R. Aaij *et al.* [LHCb Collaboration], Nucl. Phys. B 871, 1 (2013)) at $2.5 < y < 3$ and ATLAS (G. Aad *et al.* [ATLAS Collaboration], Nucl. Phys. B 864, 341 (2012)) at $|\eta| < 2.5$ respectively. The curves show the extent of the theoretical uncertainty bands. The HVQMNR code (blue dashed curves) utilizes $(\langle k_T^2 \rangle (\mathrm{GeV}^2), \epsilon_P) = (1.5, 0.008)$ for charm and (3,0.0004) for bottom. The corresponding FONLL uncertainty band (red curves) is also shown. The same quark mass and scale parameters are used in both calculations.**

Fragmentation and Broadening Effects on $\Delta\phi$

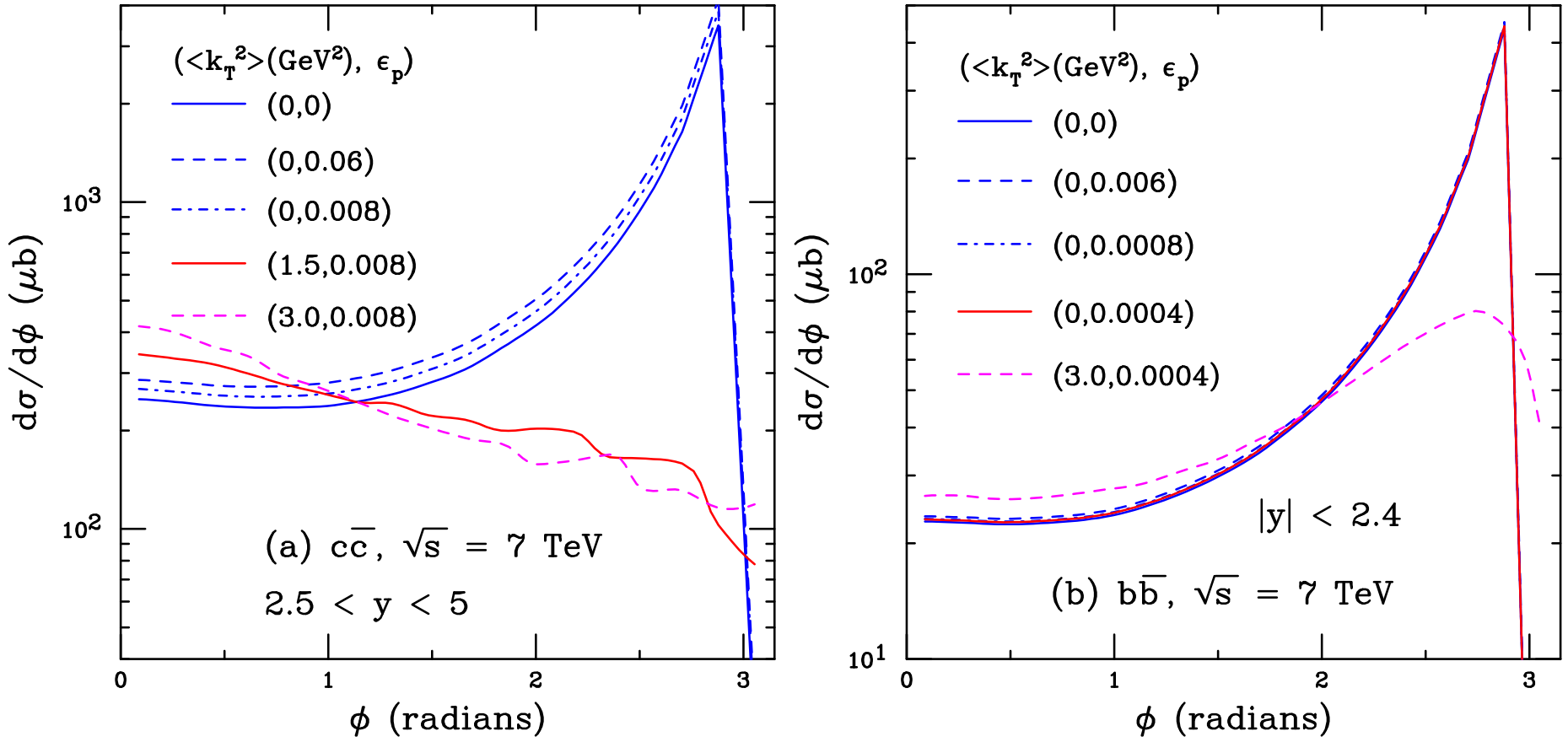

Figure 11: **The NLO azimuthal distribution between two heavy quarks, $d\sigma/d\phi$ in $p+p$ collisions at $\sqrt{s} = 7$ TeV using the HVQMNR code for (a) $c\bar{c}$ pairs at forward rapidity, $2.5 < y < 5$, and (b) $b\bar{b}$ pairs at midrapidity, $|y| < 2.4$. The results are shown for various choices of $\langle k_T^2 \rangle$ and ϵ_P.**

Sensitivity of Results

Studied sensitivity of azimuthal correlations on $\langle k_T^2 \rangle$ and p_T cut

$$k_T^2 = 1 + \frac{\Delta}{n} \ln\left(\frac{\sqrt{s}}{20\,\mathrm{GeV}}\right)\ \mathrm{GeV}^2$$

Studied $\Delta = -3/2, -1, -1/2, 0, 1/2, 1$ for c, $-1/2, 0, 1/2, 1$ for b

Low p_T is most sensitive to k_T in azimuthal correlation

Effect is independent of rapidity

Charm Pairs, $p_T < 10$ GeV

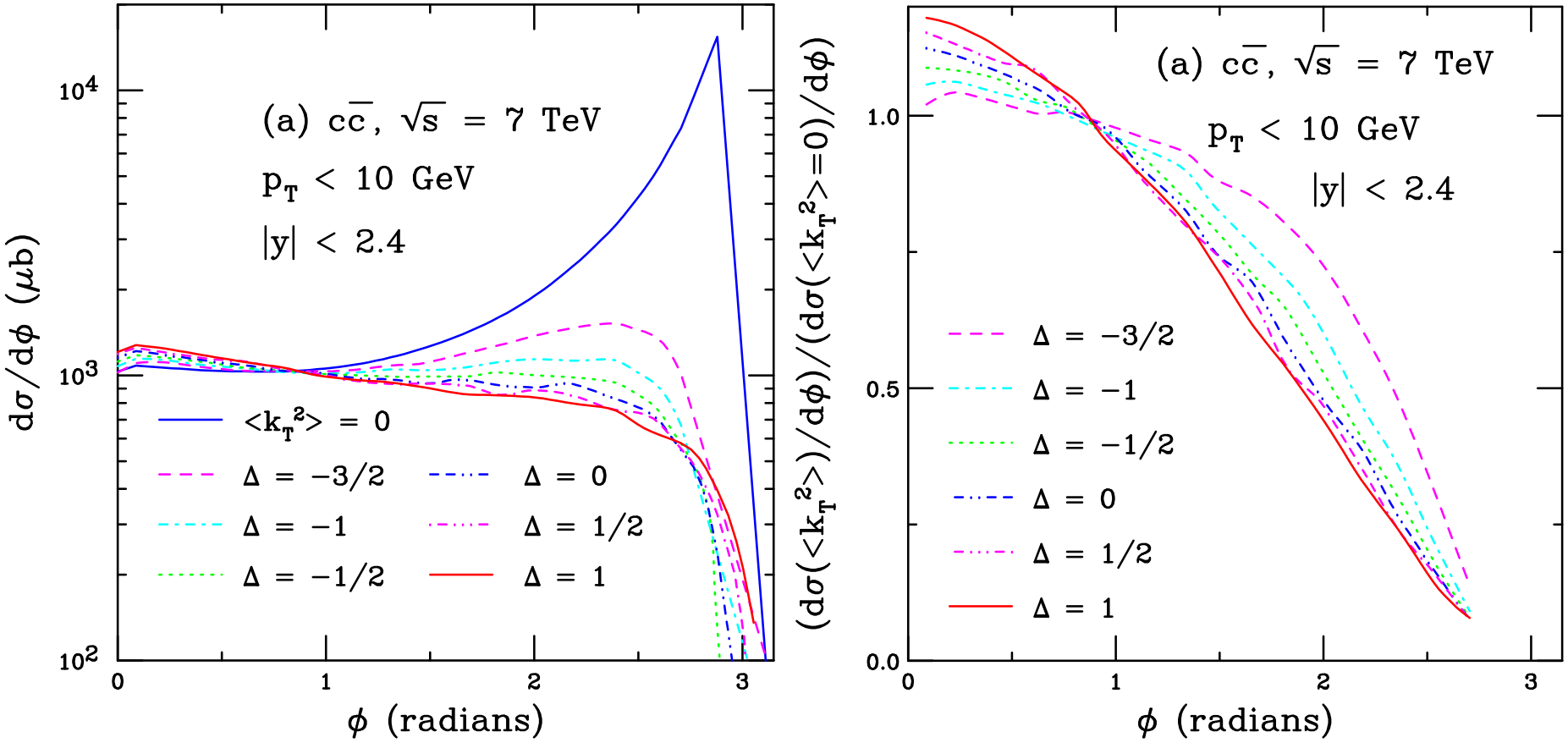

Figure 12: **The azimuthal angle distributions (left) and ratios relative to $\langle k_T^2 \rangle = 0$ (right) for $c\bar{c}$ in the central rapidity range $|y| < 2.4$ with $p_T < 10$ GeV. Calculations are shown with $\langle k_T^2 \rangle = 0$ and for values of Δ from $-3/2$ to 1.**

Charm Pairs, $p_T > 10$ GeV

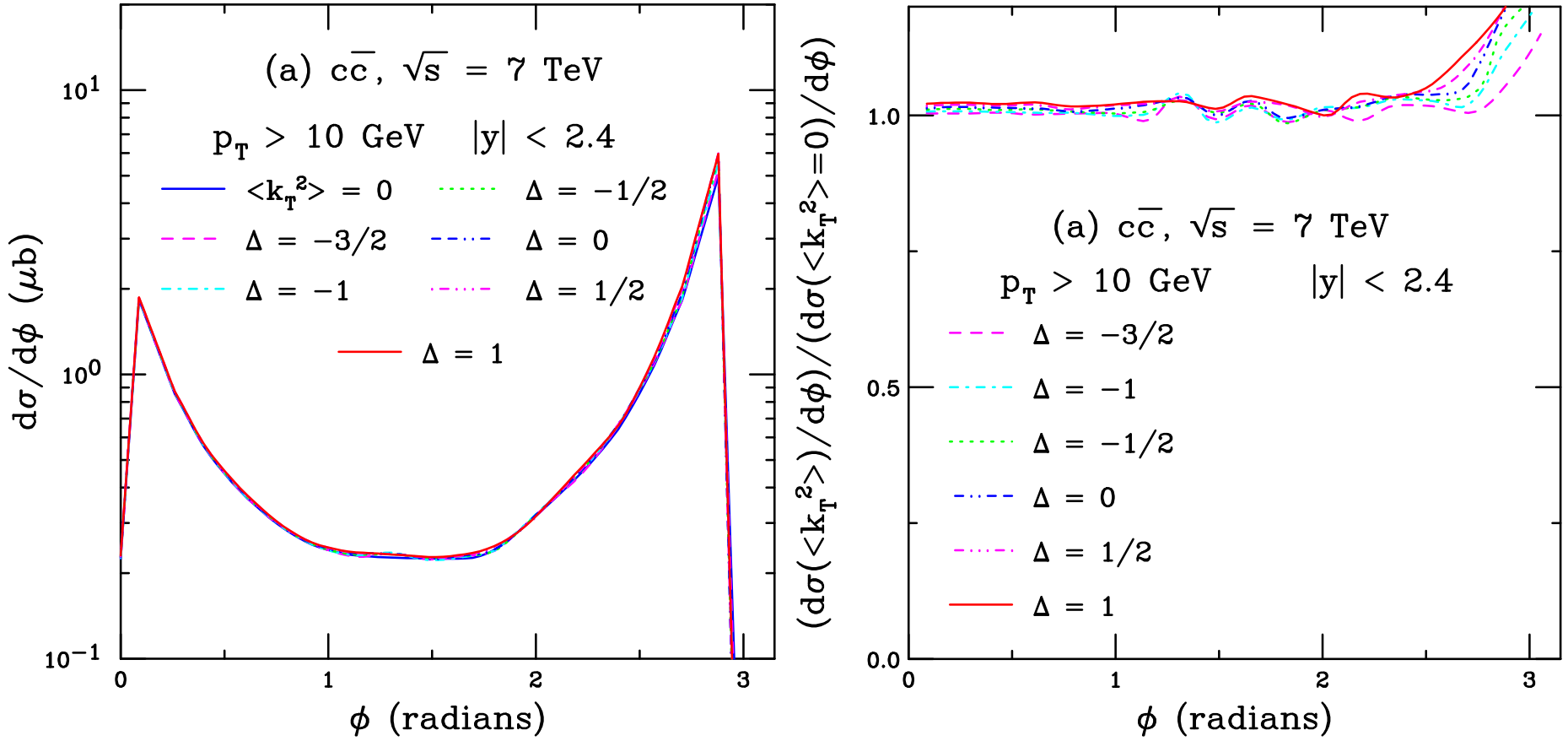

Figure 13: **The azimuthal angle distributions (left) and ratios relative to $\langle k_T^2 \rangle = 0$ (right) for $c\bar{c}$ in the central rapidity range $|y| < 2.4$ with $p_T > 10$ GeV. Calculations are shown with $\langle k_T^2 \rangle = 0$ and for values of Δ from $-3/2$ to 1.**

Bottom Pairs, $p_T < 10$ GeV

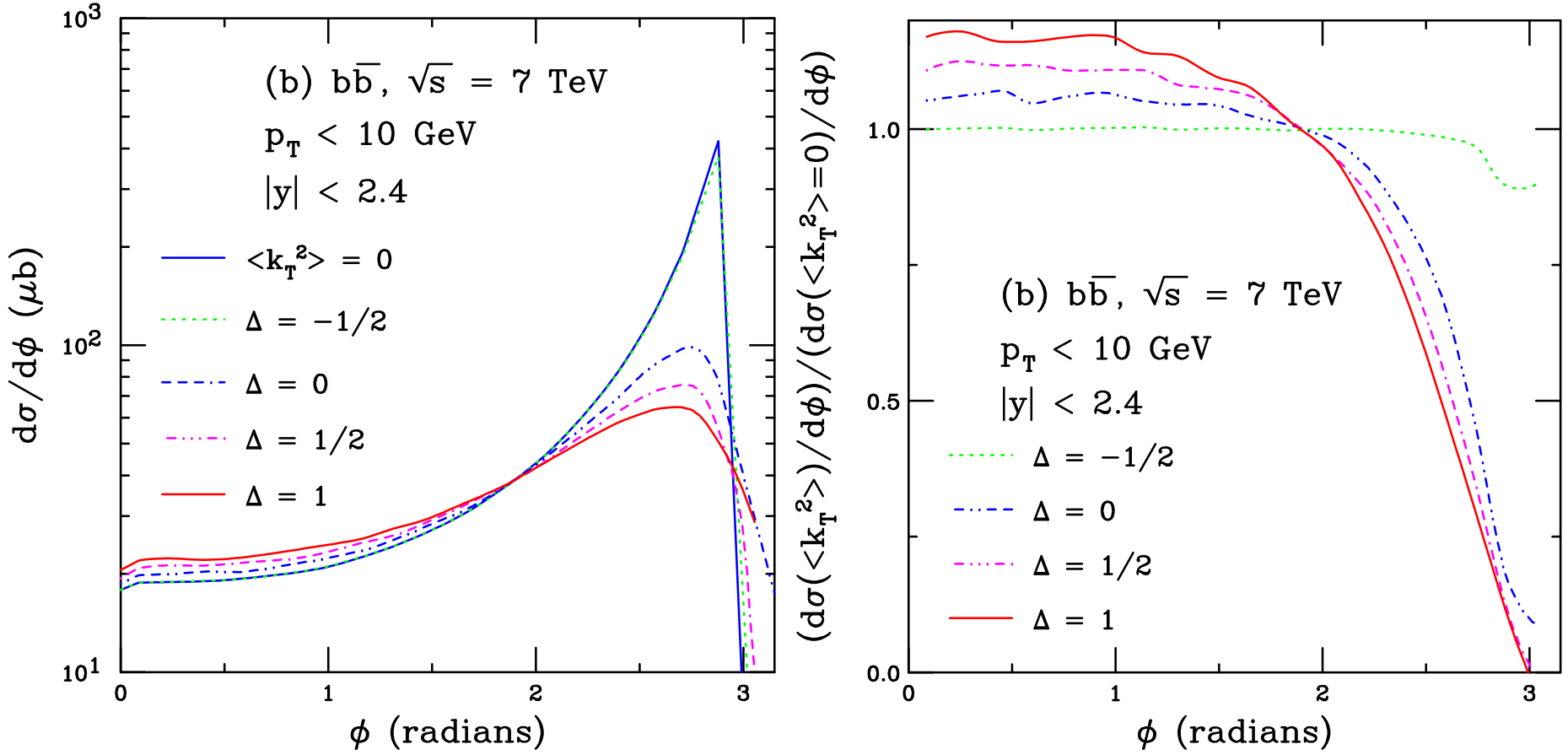

Figure 14: **The azimuthal angle distributions (left) and ratios relative to $\langle k_T^2 \rangle = 0$ (right) for $b\bar{b}$ in the central rapidity range $|y| < 2.4$ with $p_T < 10$ GeV. Calculations are shown with $\langle k_T^2 \rangle = 0$ and for values of Δ from $-1/2$ to 1.**

Bottom Pairs, $p_T > 10$ GeV

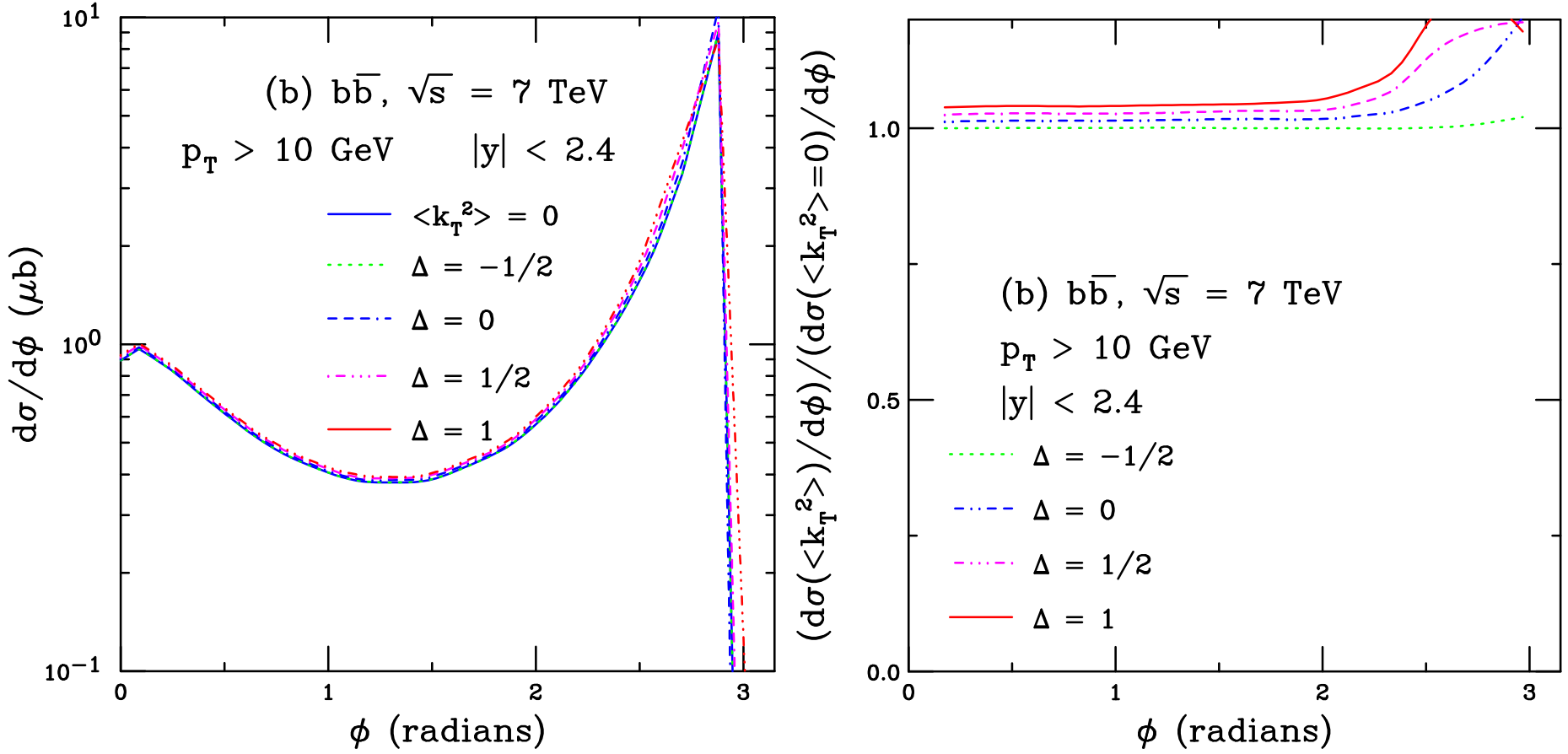

Figure 15: **The azimuthal angle distributions (left) and ratios relative to $\langle k_T^2 \rangle = 0$ (right) for $b\bar{b}$ in the central rapidity range $|y| < 2.4$ with $p_T > 10$ GeV. Calculations are shown with $\langle k_T^2 \rangle = 0$ and for values of Δ from $-1/2$ to 1.**

LHCb Measured Charm Pair Correlations

Measured cc (D^+D^+) and $c\bar{c}$ (D^+D^-) pairs

10 times more $c\bar{c}$ events than cc, more isotropic in $\Delta\phi$ and harder pair p_T distributions

cc events likely due to double parton scattering

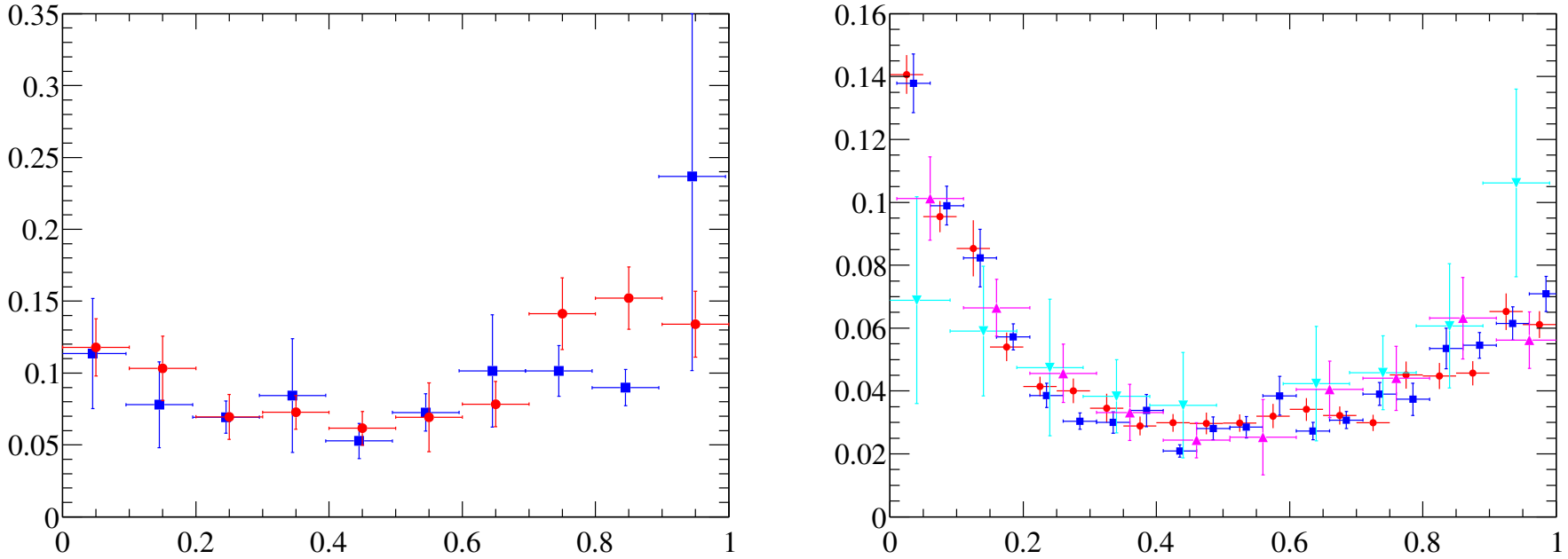

Figure 16: **(Left)** cc $\Delta\phi/\pi$. **(Right)** $c\bar{c}$ $\Delta\phi/\pi$. **Both measured at $\sqrt{s} = 7$ TeV by LHCb [R. Aaij *et al.* [LHCb Collaboration], JHEP 1206, 141 (2012), [JHEP 1403, 108 (2014)]].**

Charm $\Delta\phi$ Distributions Compared to CDF and LHCb

CDF: $p_T > 5.5$ GeV for D^0, D^{*-} and 7 GeV for D^+

LHCb: $p_T > 3$ GeV for $D\overline{D}$ pairs

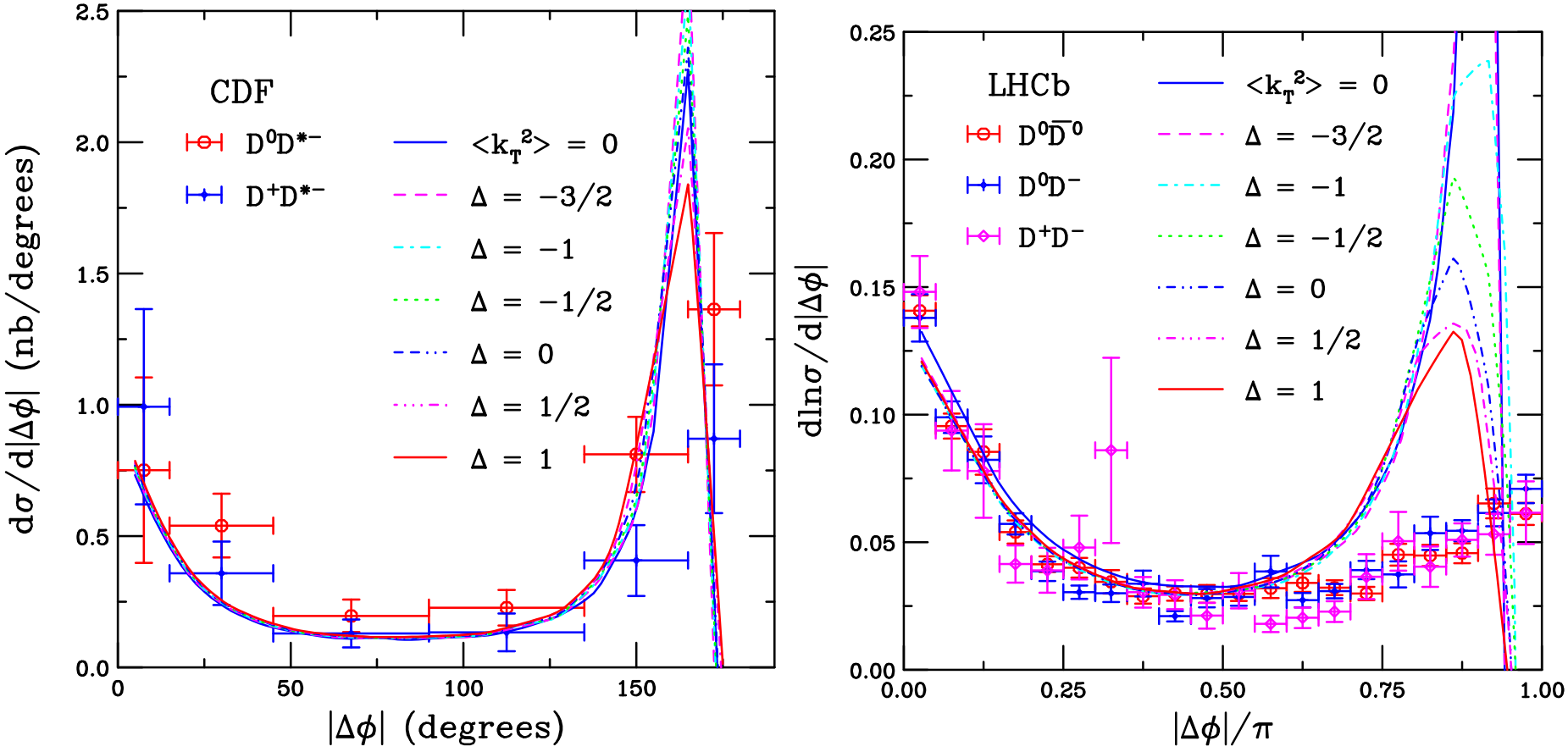

Figure 17: **(Left) The azimuthal angle distributions for D^0D^{*-} (red) and D^+D^{*-} (blue) pairs measured in $p+\overline{p}$ collisions at $\sqrt{s} = 1.96$ TeV by CDF [B. Reisert *et al.* [CDF Collaboration], Nucl. Phys. Proc. Suppl. 170, 243 (2007)]. The data are compared to calculations in the same acceptance with $\langle k_T^2 \rangle = 0$ and for values of Δ from $-3/2$ to 1. (Right) The azimuthal angle distributions for $D^0\overline{D}^0$ (red), D^0D^- (blue), and D^+D^- (magenta) pairs measured in $p+p$ collisions at $\sqrt{s} = 7$ TeV by LHCb [R. Aaij *et al.* [LHCb Collaboration], JHEP 1206, 141 (2012), [JHEP 1403, 108 (2014)]] The data are compared to calculations in the same acceptance with $\langle k_T^2 \rangle = 0$ and for values of Δ from $-3/2$ to 1.**

LHCb Also Measured $c\bar{c}$ Mass and Δy Distributions

Mass distributions favor finite k_T kick with $\Delta = 1$

Δy distributions do not depend on k_T kick, as expected

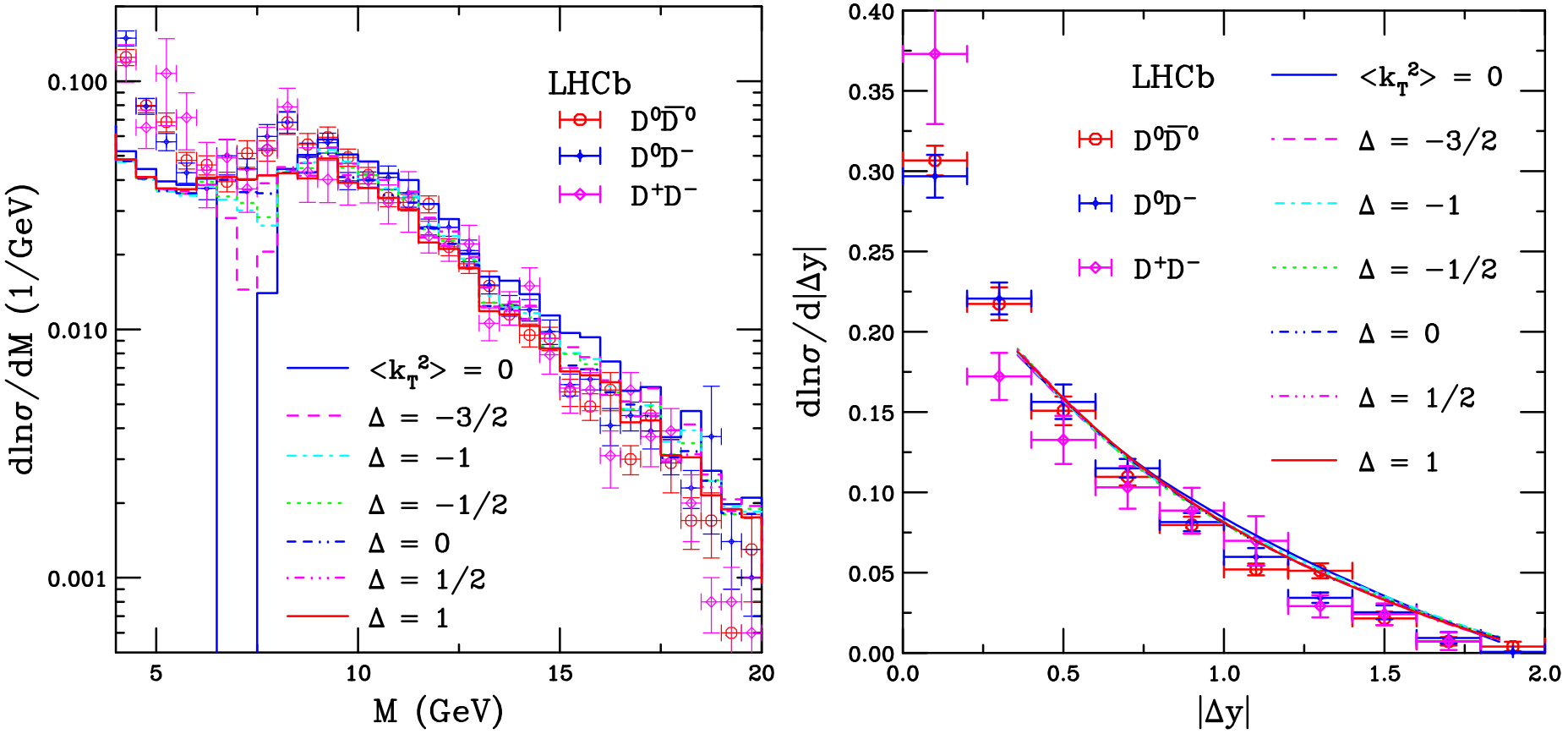

Figure 18: **(Left) $c\bar{c}$ pair mass. (Right) Δy for $c\bar{c}$. From [R. Aaij *et al.* [LHCb Collaboration], JHEP 1206, 141 (2012), [JHEP 1403, 108 (2014)]] The data are compared to calculations in the same acceptance with $\langle k_T^2 \rangle = 0$ and for values of Δ from $-3/2$ to 1.**

LHC $b\bar{b} \to J/\psi J/\psi$ Correlations

LHCb measured $b\bar{b} \to J/\psi J/\psi$ at $\sqrt{s} = 7$ and 8 TeV (R. Aaij *et al.* (LHCb Collaboration), JEHP 11 (2017) 030)

Presented results for six pair observables:

- **$|\Delta\phi^*|$, the difference in azimuthal angle between the b and $\bar{b}$ mesons, also $|\Delta\phi|$, the azimuthal opening angle between the two J/ψs**
- **$|\Delta\eta^*|$, the difference in pseudorapidity between the b and $\bar{b}$ mesons and $|\Delta\eta|$ between the two J/ψs**
- **A_T, the asymmetry between the transverse momenta of the J/ψs**
- **Mass, M, of the J/ψ pair**
- **J/ψ pair transverse momentum, p_{T_p}**
- **J/ψ piar rapidity, y_p**

Each observable was studied with four different p_T cuts: $p_T > 2$, 3, 5 and 7 GeV

All the pair observables studied by LHCb will be calculated for both the parent $b\bar{b}$ mesons and the subsequent $J/\psi J/\psi$ decays.

Azimuthal Distributions, $|\Delta\phi^*|$ and $|\Delta\phi|$

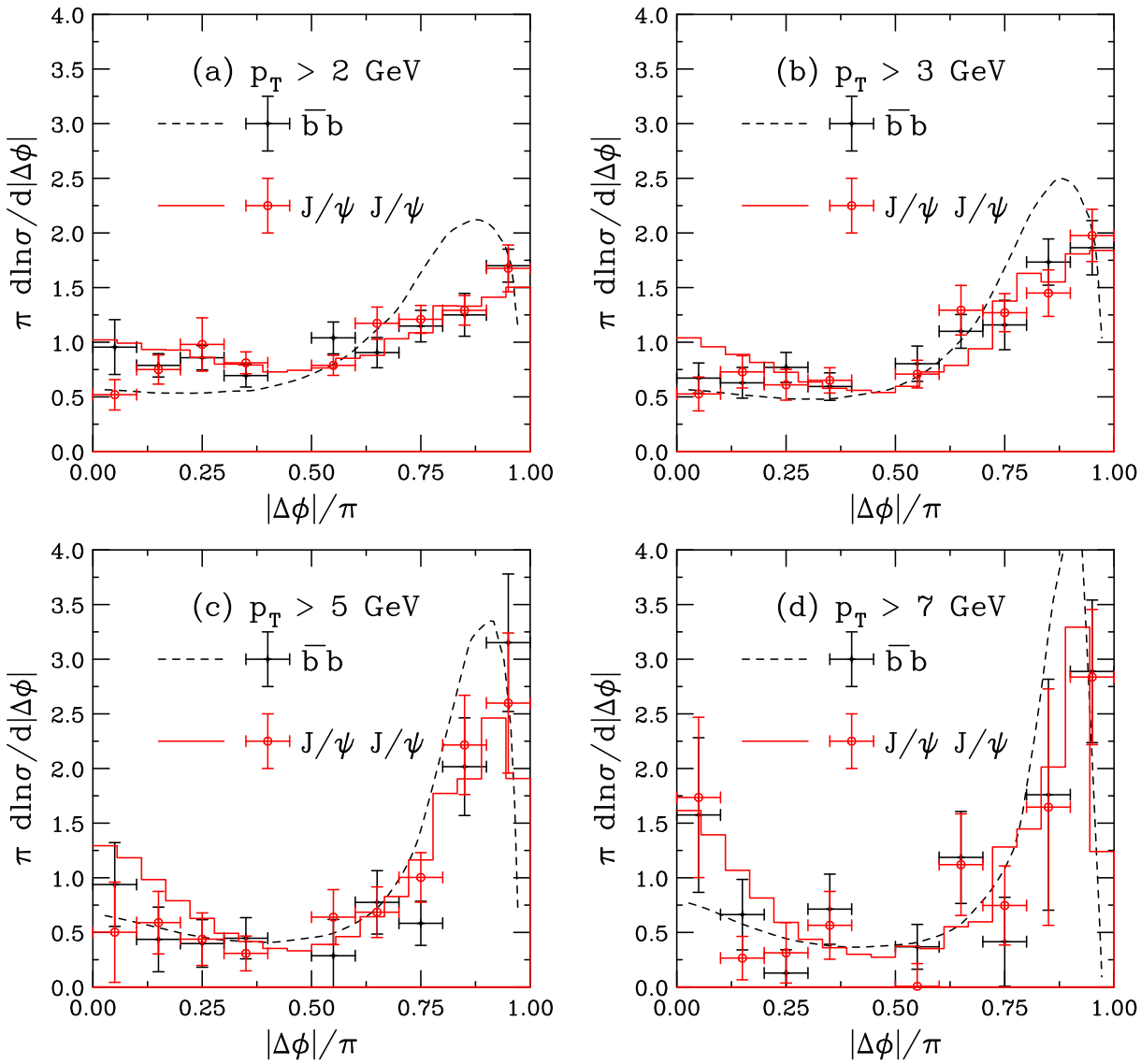

Figure 19: **The azimuthal angle difference between the b and $\bar{b}$ (black dashed curves) and the J/ψ's resulting from B decays (red histograms) are compared to the LHCb data (black: $b\bar{b}$, red circles: J/ψ pairs) for p_T cuts on the B and the J/ψ of 2 (a), 3 (b), 5 (c) and 7 GeV (d).**

Rapidity Difference, $|\Delta y^*|$ and $|\Delta y|$

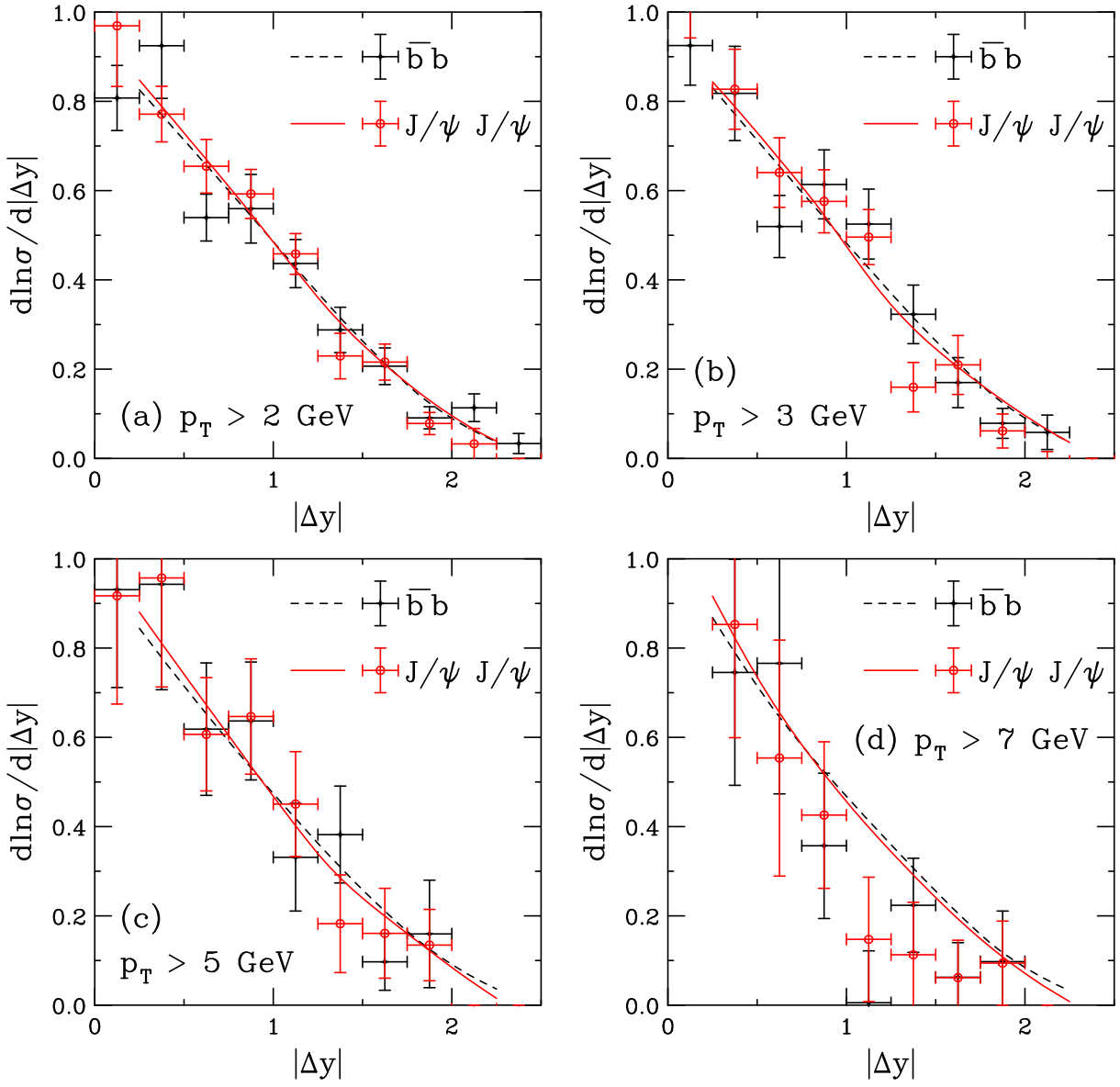

Figure 20: **The rapidity difference $|\Delta y|$ between the b and $\overline{b}$ (black dashed curve) and the J/ψ's resulting from B decays (red solid curve) are compared to the LHCb data (black: $b\overline{b}$, red circles: J/ψ pairs) for p_T cuts on the B and the J/ψ of 2 (a), 3 (b), 5 (c) and 7 GeV (d).**

Pair Mass Distributions, M

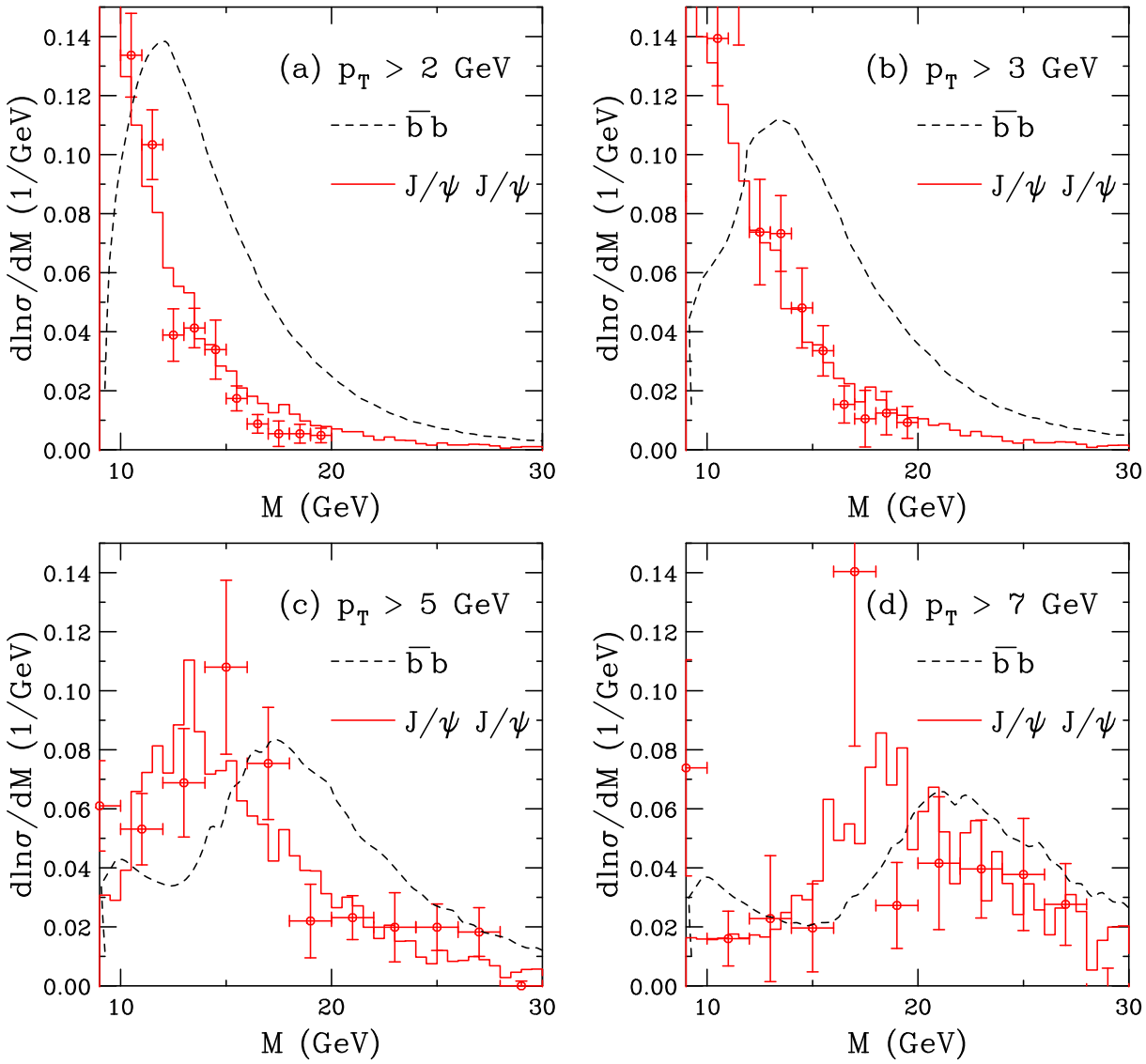

Figure 21: **The pair mass of the b and $\bar{b}$ (black dashed lines) and the J/ψ's resulting from B (red histograms) are compared to the LHCb data (red circles) for p_T cuts on the B and the J/ψ of 2 (a), 3 (b), 5 (c) and 7 GeV (d).**

Pair Rapidity Distributions, y_p

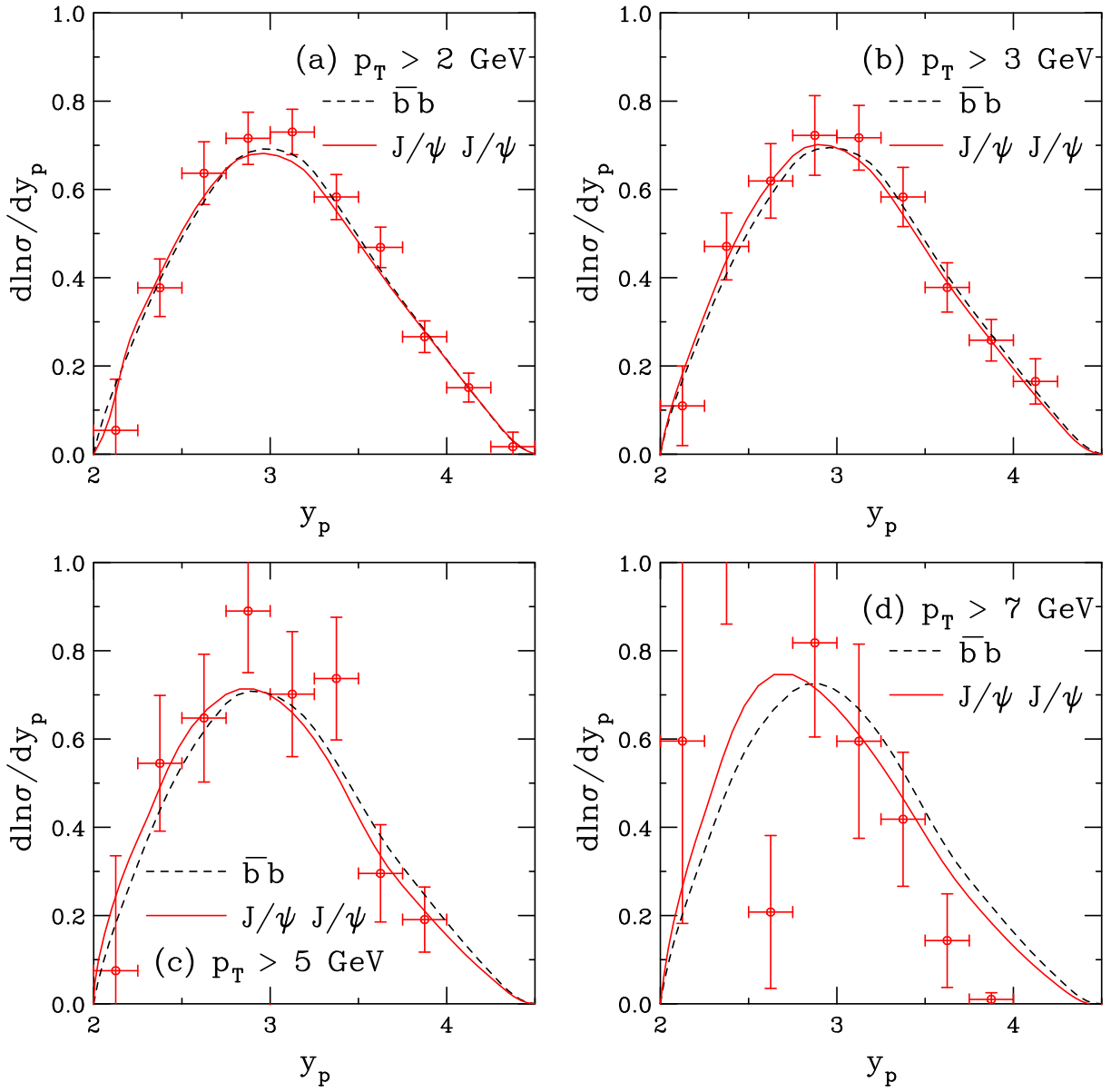

Figure 22: **The pair rapidity of the b and $\overline{b}$ (black dashed curves) and the J/ψ's resulting from B decays (red solid curves) are compared to the LHCb data (red circles) for p_T cuts on the B and the J/ψ of 2 (a), 3 (b), 5 (c) and 7 GeV (d).**

Switching Gears: Nuclear Matter Effects in $p + A$

Cold and Hot Nuclear Matter Effects on Charm $R_{p\mathrm{Pb}}$

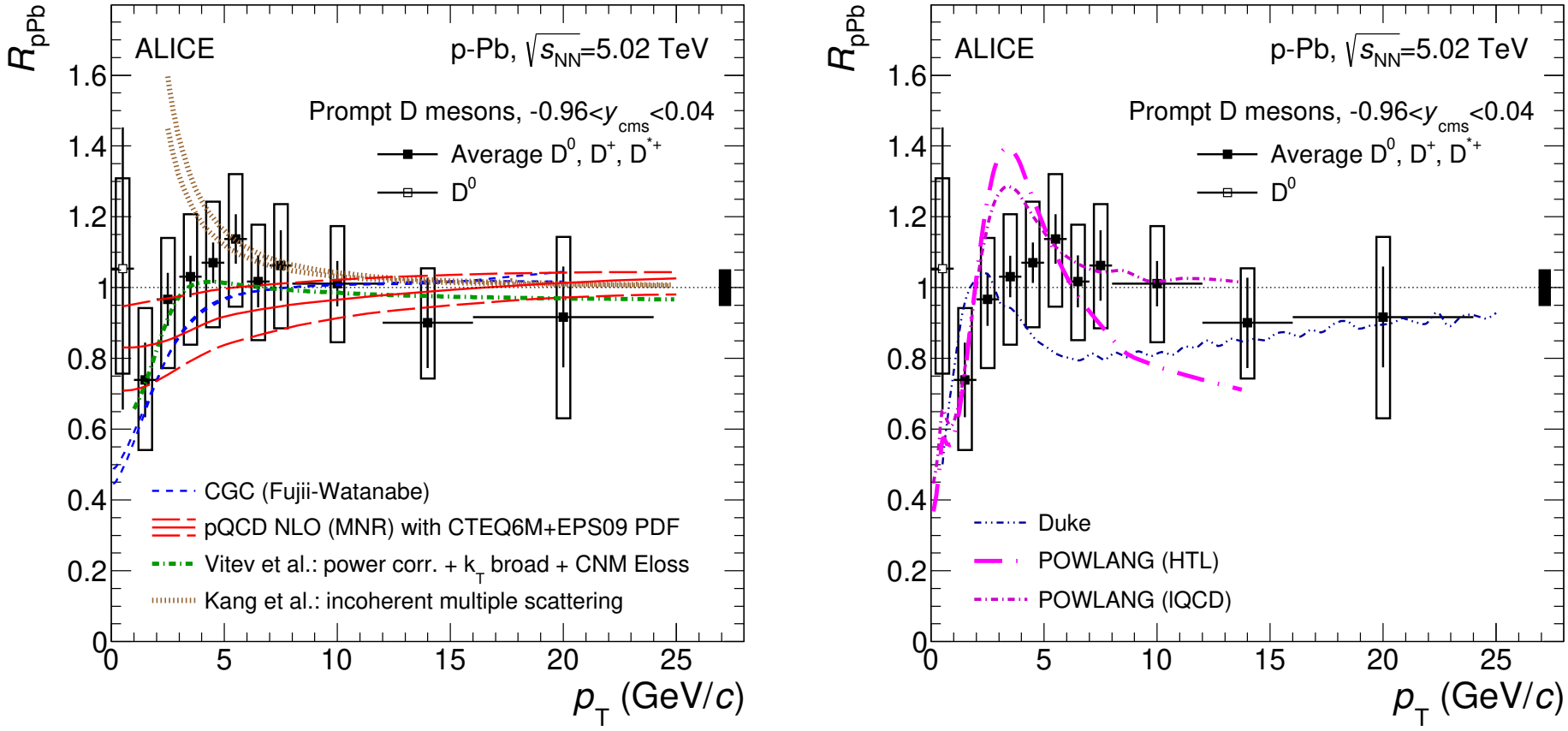

Figure 23: **The nuclear modification factor $R_{p\mathrm{Pb}}(p_T)$ in 5.02 TeV p+Pb collisions for $-0.96 < y_{\mathrm{cm}} < 0.04$. (Left) Models of cold nuclear matter only. (Right) Calculations that include medium effects are shown. From the ALICE Collaboration, Phys. Rev. C 94, 054908 (2016).**

Charm in pA at $\sqrt{s_{NN}} = 5$ TeV, This Model

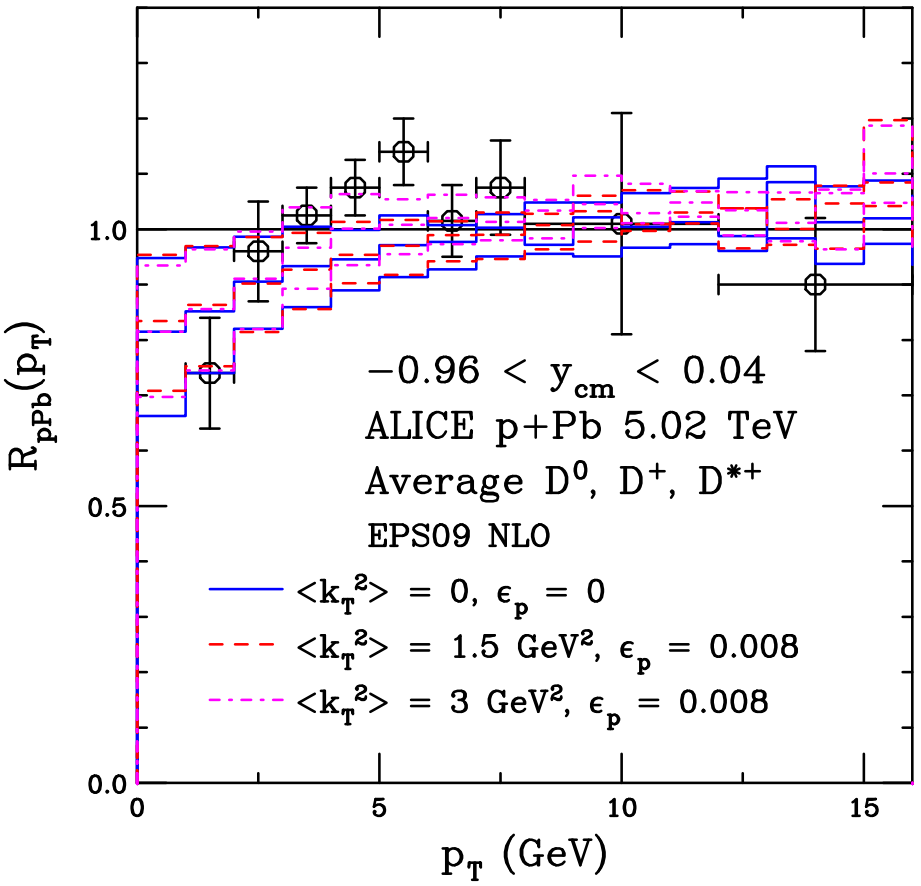

Figure 24: **(Left) The nuclear modification factor $R_{p\mathrm{Pb}}(p_T)$ in 5.02 TeV p+Pb collisions for $-0.96 < y_{\mathrm{cm}} < 0.04$. The ALICE data for the average of their D^0, D^+ and D^{*+} measurements (B. Abelev *et al.* [ALICE Collaboration], Phys. Rev. Lett. 113, 232301 (2014)) at central rapidity are shown. Results are shown for: noThe nuclear modification factor $R_{p\mathrm{Pb}}(\phi)$ in 5.02 TeV p+Pb k_T broadening and no fragmentation (solid blue); $\langle k_T^2 \rangle = 1.5$ GeV^2 and $\epsilon_P = 0.008$ (red dashed); and $\langle k_T^2 \rangle = 3$ GeV^2 and $\epsilon_P = 0.008$ (magenta dot-dashed). The EPS09 NLO uncertainty band, along with the central value, is shown. Note that the additional k_T broadening is only applied to p+Pb collisions and not to $p+p$ collisions in the magenta curves.**

CNM Effects on Single Bottom p_T Distributions

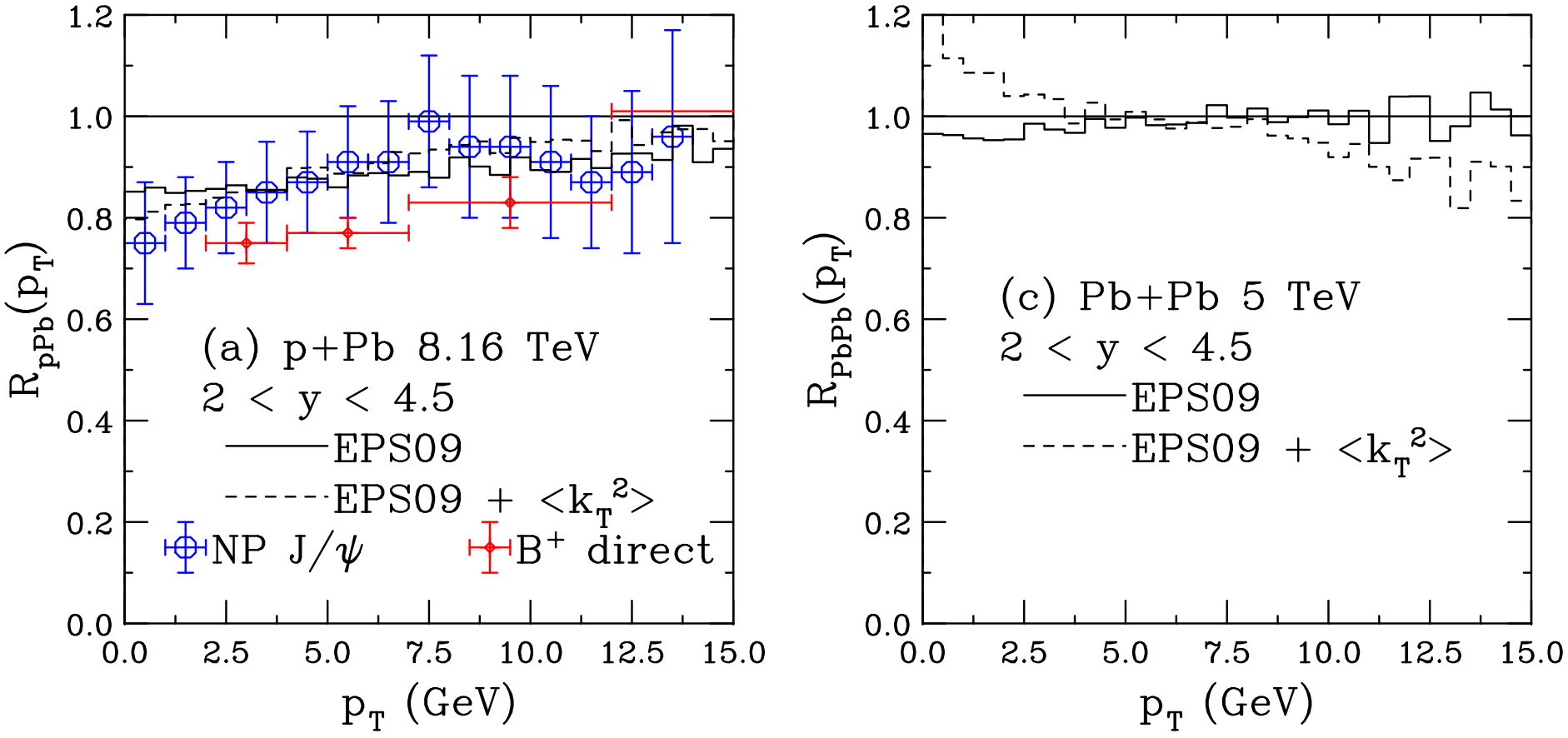

Figure 25: **Cold nuclear matter effects on b quark p_T distributions for (a) p+Pb collisions at 8.16 TeV with central EPS09 and the same k_T kick as in $p+p$ (solid) and additional k_T broadening in Pb (dashed); (c) Pb+Pb collisions at 5 TeV with central EPS09 with the same k_T kick in $p+p$ and Pb+Pb (solid) and additional k_T broadening in the Pb nuclei with a modified fragmentation function in Pb (dashed). In (a) the calculations are compared to the LHCb data on non-prompt J/ψs (R. Aaij *et al.* [LHCb Collaboration], Phys. Lett. B 774, 159 (2017).) and direct B^+ (R. Aaij *et al.* [LHCb Collaboration], Phys. Rev. D 99, 052011 (2019).).**

Nuclear Matter Effects on Pair Observables

- **Schematically studied $b\bar{b}$ pair observables with different p_T cuts by:**
  - **Introducing additional broadening for Cronin effects in $p + A$ and $A + A$**
  - **Reverted to default Peterson fragmentation parameter to simulate energy loss in $A + A$**
- **Note that the effects would be more pronounced for $c\bar{c}$ because of the lower mass**

Nuclear Matter Effects Included

- **Nuclear modification of parton densities (shadowing) changes parton distributions in the nucleus:** $f_i^A(x,Q^2) = S_i^A(x,Q^2) f_i^p(x,Q^2)$ **where** f_i **is the parton density** ($i = q$, $\overline{q}$ **or** g) **and** S_i^A **is the shadowing factor, determined from global analyses**

- **Cronin effect modeled by enhanced** k_T **broadening in the nucleus:**

$$k_T^2 = 1 + \frac{\Delta}{n} \ln\left(\frac{\sqrt{s}}{20\,\mathrm{GeV}}\right)\ \mathrm{GeV}^2 \quad [pA : \Delta = 2,\ \ AA : \Delta = 4]$$

- **Energy loss modeled by assuming that the fragmentation parameter is increased:** ϵ_P **is taken to be the** e^+e^- **value in** AA **collisions**

Implementation on $b\bar{b}$ Pairs

- **Nuclear modification of parton densities (shadowing) only in pA and AA**
- **Shadowing plus additional broadening ($\Delta = 2$) in pA**
- **Shadowing, additional broadening ($\Delta = 4$), and increased ϵ_P in AA**
- **pA calculated at $\sqrt{s_{NN}} = 8.16$ TeV; AA at $\sqrt{s_{NN}} = 5.02$ TeV; pp calculated at the same energies**
- **Results shown only for forward rapidities, similar dependence at central rapidity, see paper for more details**
- **Studied pair quantities $|\Delta\phi|$ and y_p**

The results for pair rapidities are more sensitive to changes in fragmentation while azimuthal effects are more sensitive to enhanced k_T broadening

Sensitivity to transverse momentum studied by employing the same p_T cuts as LHCb $b\bar{b} \to J/\psi J/\psi$ studies, B $p_T > 2$, 3, 5 and 7 GeV

Energy and Matter Dependence of Pair Rapidity

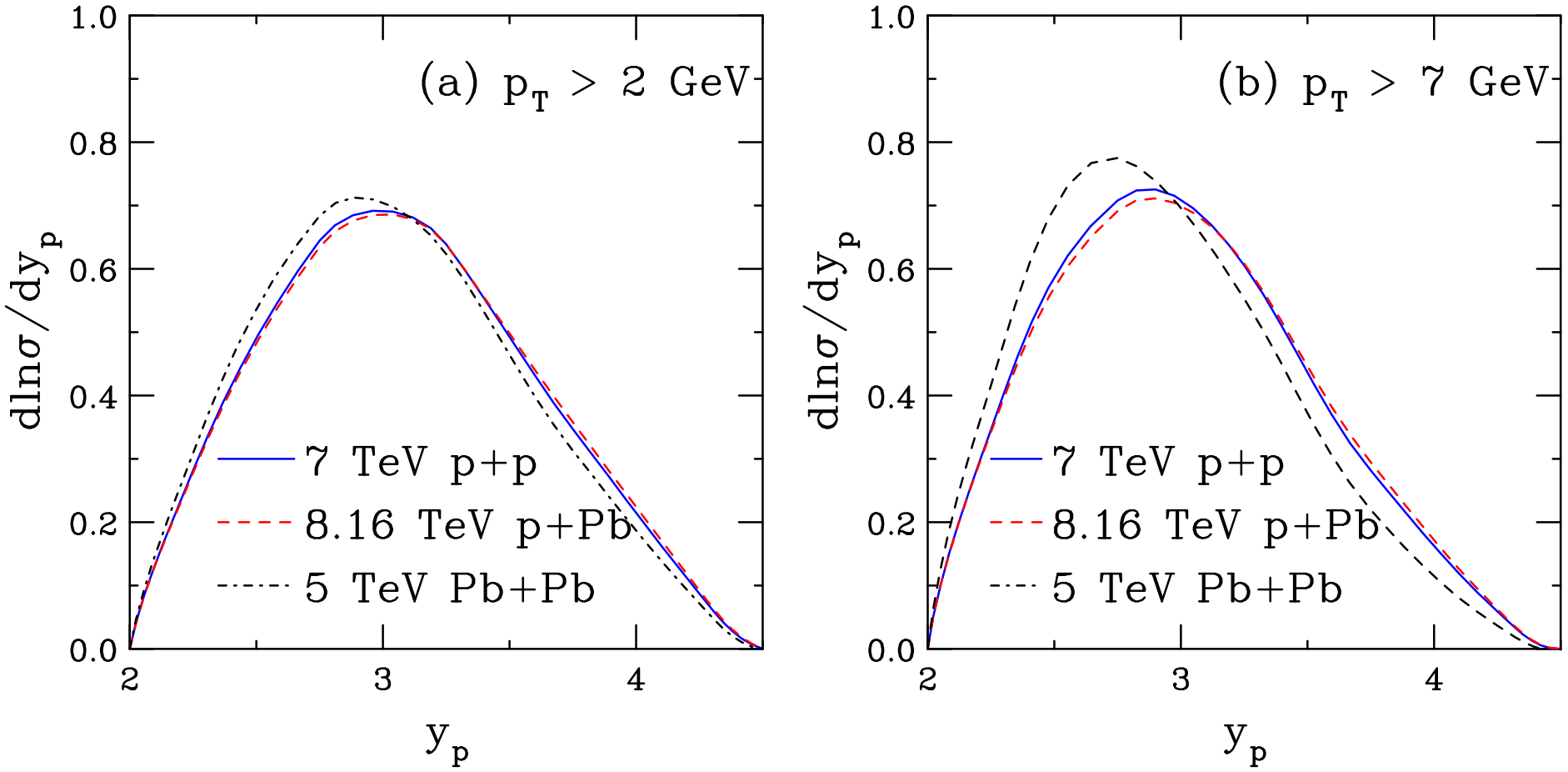

Figure 26: **The $b\bar{b}$ pair rapidity in the range $2 < y_p < 4.5$ for $p_T > 2$ (a) and 7 GeV (b) for $p+p$ collisions at 7 TeV (solid blue), p+Pb collisions at 8.16 TeV (dashed red) and Pb+Pb collisions at 5 TeV (dot-dashed black). The p+Pb calculations include shadowing and enhanced broadening (2Δ) while the Pb+Pb calculations include shadowing, broadening (4Δ), and fragmentation function modification.**

Modification of Pair Rapidity Distributions

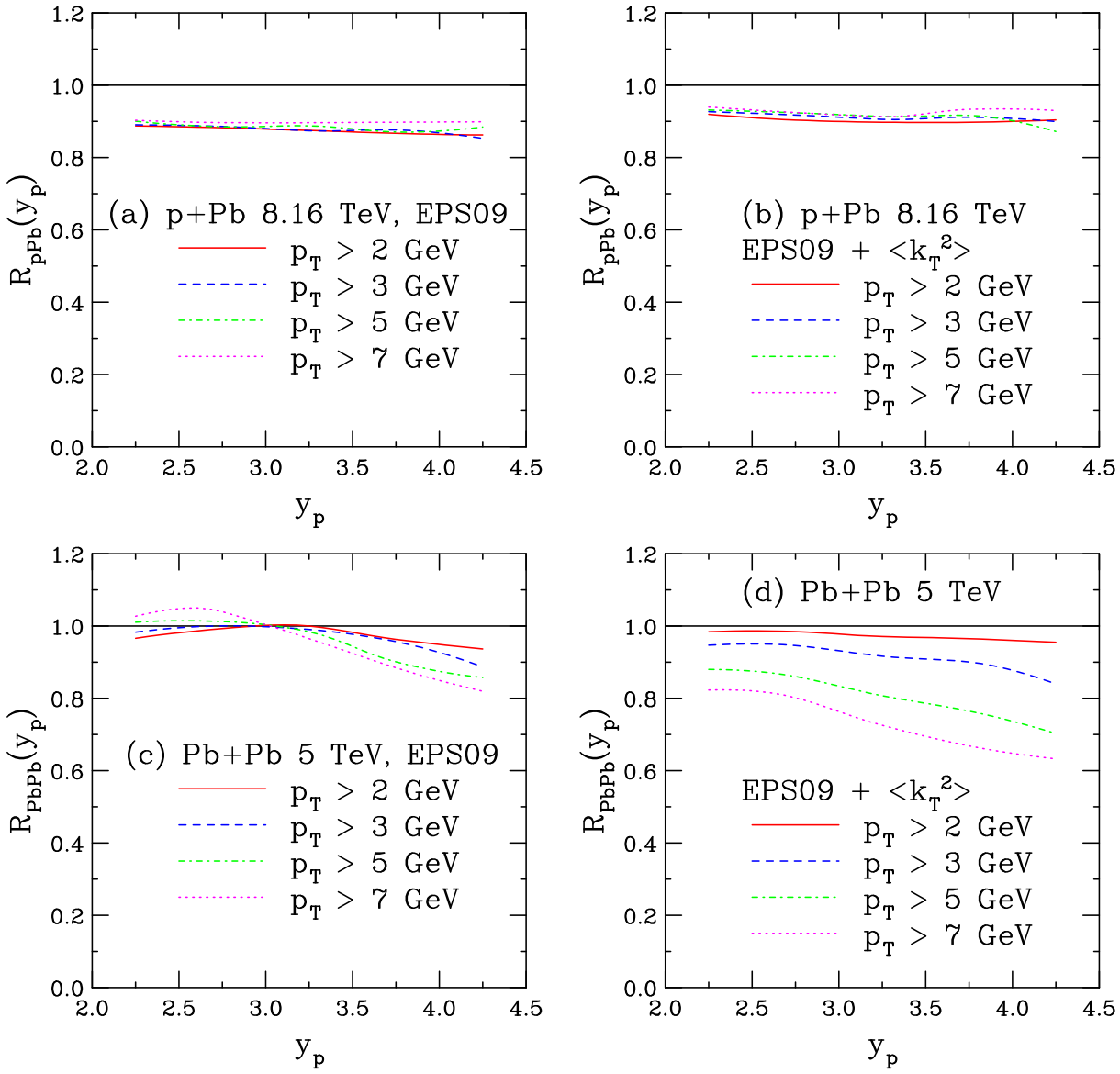

Figure 27: **Cold nuclear matter effects in $2 < y < 4.5$ on the $b\bar{b}$ pair rapidity for $p_T > 2$ (solid red), 3 (dashed blue), 5 (dot-dashed green), and 7 GeV (dotted magenta) for (a) p+Pb collisions at 8.16 TeV with central EPS09 and the same k_T kick as in $p+p$; (b) $R_{p\mathrm{Pb}}$ at 8.16 TeV with EPS09 and additional k_T broadening in Pb; (c) Pb+Pb collisions at 5 TeV with central EPS09 with the same k_T kick in $p+p$ and p+Pb; and (d) R_{AA} at 5 TeV with EPS09, additional k_T broadening in the Pb nuclei, and a modified fragmentation function in Pb.**

Energy and Matter Dependence of $|\Delta\phi|$

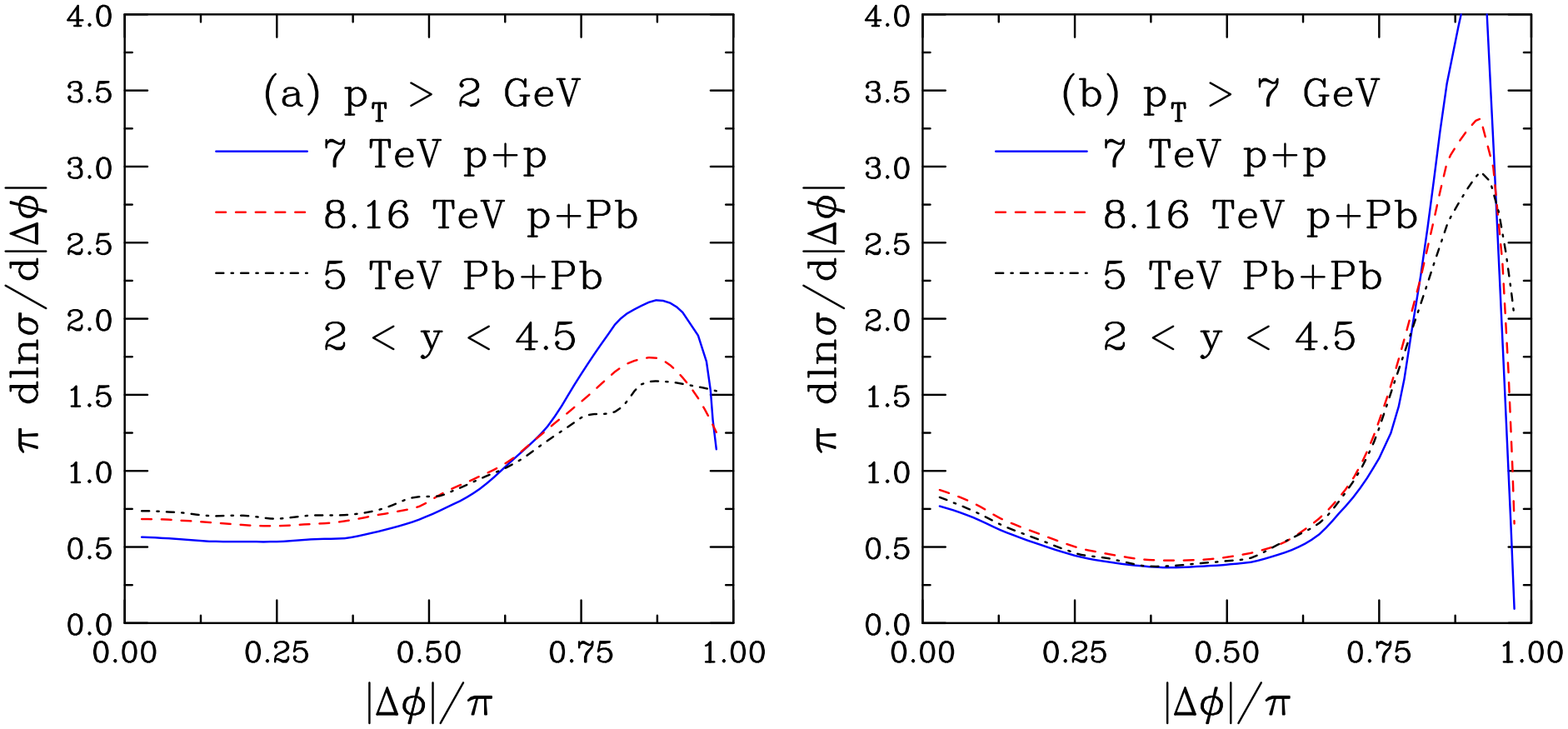

Figure 28: **The $b\bar{b}$ azimuthal difference in the range $2 < y_p < 4.5$ for $p_T > 2$ (a) and 7 GeV (b) for $p + p$ collisions at 7 TeV (solid blue), p+Pb collisions at 8.16 TeV (dashed red) and Pb+Pb collisions at 5 TeV (dot-dashed black). The p+Pb calculations include shadowing and enhanced broadening (2Δ) while the Pb+Pb calculations include shadowing, broadening (4Δ), and fragmentation function modification.**

Modification of Azimuthal Distributions

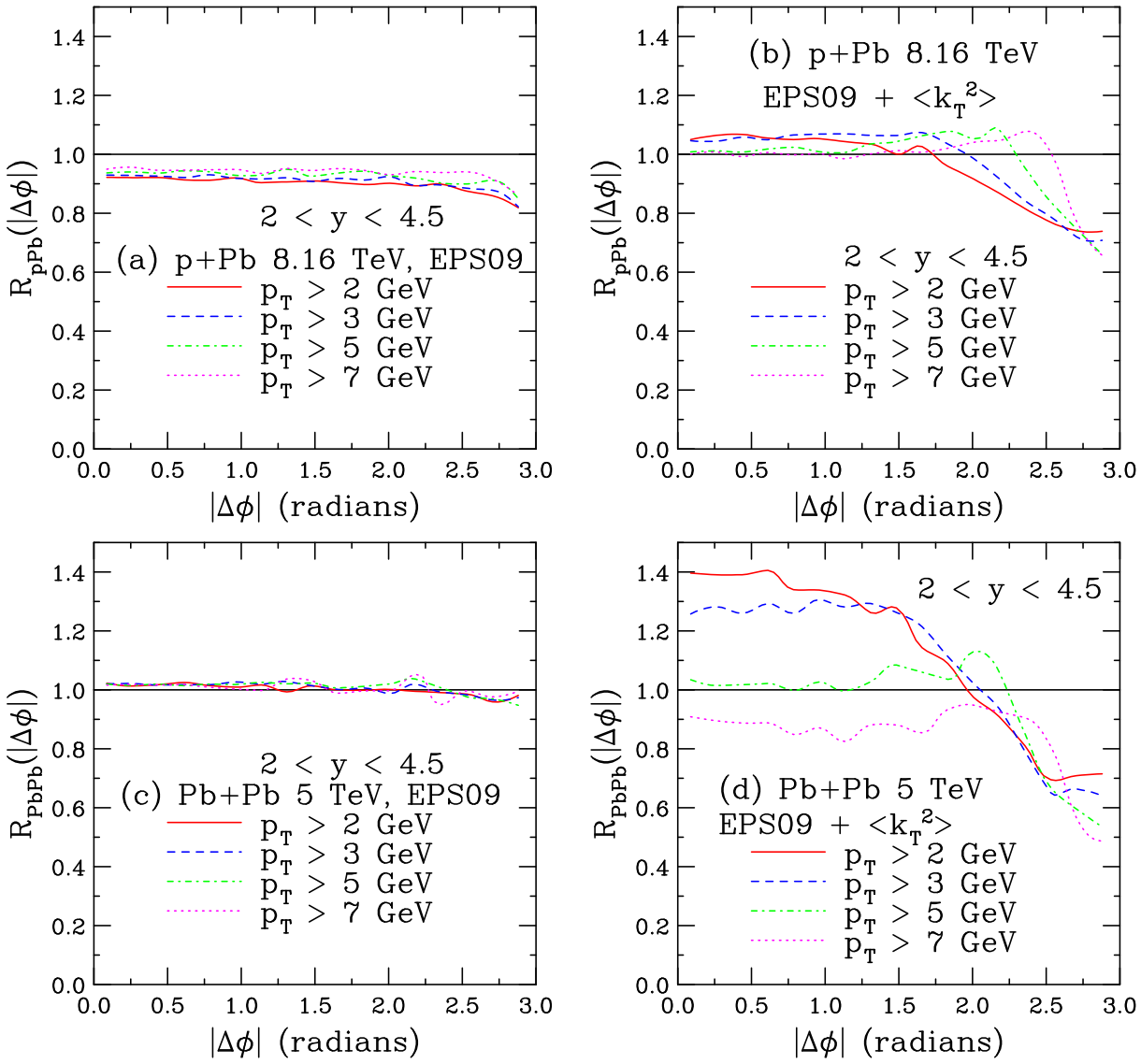

Figure 29: **Cold nuclear matter effects at forward rapidity ($2 < y < 4.5$) on the $b\bar{b}$ azimuthal angle difference for $p_T > 2$ (solid red), 3 (dashed blue), 5 (dot-dashed green), and 7 GeV (dotted magenta) for (a) p+Pb collisions at 8.16 TeV with central EPS09 and the same k_T kick as in $p+p$; (b) $R_{p\mathrm{Pb}}$ at 8.16 TeV with EPS09 and additional k_T broadening in Pb; (c) Pb+Pb collisions at 5 TeV with central EPS09 with the same k_T kick in $p+p$ and p+Pb; and (d) R_{AA} at 5 TeV with EPS09, additional k_T broadening in the Pb nuclei and a modified fragmentation function in Pb.**

Summary

- **Single particle heavy flavor observables provide limited information**
- **Heavy quark pair observables are harder to measure but can provide more constraints on models and more detailed information**
- **Heavy quark pair correlations in $p+p$ and $p\overline{p}$ collisions can be explained by NLO heavy flavor production processes**
- **$p+p$ results are most sensitive to k_T broadening at low p_T, practically insensitive to fragmentation/hadronization**
- **Effects on pair observables sensitive to hot and cold nuclear matter effects; illustrative results here show that pair rapidity is sensitive to energy loss while azimuthal angle separation is sensitive to Cronin-like p_T broadening effects**

Open Charm and Bottom Hadrons

$C_{\rm had}$	**Mass (GeV)**	$c\tau$ **(μm)**	$B(C_{\rm had} \to lX)$ **(%)**	$B(C_{\rm had} \to$ Hadrons**)** **(%)**
$D^+(c\overline{d})$	**1.869**	**315**	**17.2**	$K^-\pi^+\pi^+$ **(9.1)**
$D^-(\overline{c}d)$	**1.869**	**315**	**17.2**	$K^+\pi^-\pi^-$ **(9.1)**
$D^0(c\overline{u})$	**1.864**	**123.4**	**6.87**	$K^-\pi^+$ **(3.8)**
$\overline{D^0}(\overline{c}u)$	**1.864**	**123.4**	**6.87**	$K^+\pi^-$ **(3.8)**
$D^{*\pm}$	**2.010**			$D^0\pi^\pm$ **(67.7)**, $D^\pm\pi^0$ **(30.7)**
D^{*0}	**2.007**			$D^0\pi^0$ **(61.9)**
$D_s^+(c\overline{s})$	**1.969**	**147**	**8**	$K^+K^-\pi^+$ **(4.4)**, $\pi^+\pi^+\pi^-$ **(1.01)**
$D_s^-(\overline{c}s)$	**1.969**	**147**	**8**	$K^+K^-\pi^-$ **(4.4)**, $\pi^+\pi^-\pi^-$ **(1.01)**
$\Lambda_c^+(udc)$	**2.285**	**59.9**	**4.5**	ΛX **(35)**, $pK^-\pi^+$ **(2.8)**
$\Sigma_c^{++}(uuc)$	**2.452**			$\Lambda_c^+\pi^+$ **(100)**
$\Sigma_c^+(udc)$	**2.451**			$\Lambda_c^+\pi^0$ **(100)**
$\Sigma_c^0(ddc)$	**2.452**			$\Lambda_c^+\pi^-$ **(100)**
$B_{\rm had}$	**Mass (GeV)**	$c\tau$ **(μm)**	$B(B_{\rm had} \to lX)$ **(%)**	$B(B_{\rm had} \to$ Hadrons**)** **(%)**
$B^+(u\overline{b})$	**5.2790**	**501**	**10.2**	$\overline{D}^0\pi^-\pi^+\pi^+$ **(1.1)**, $J/\psi K^+$ **(0.1)**
$B^-(\overline{u}b)$	**5.2790**	**501**	**10.2**	$D^0\pi^+\pi^-\pi^-$ **(1.1)**, $J/\psi K^-$ **(0.1)**
$B^0(d\overline{b})$	**5.2794**	**460**	**10.5**	$D^-\pi^+$ **(0.276)**, $J/\psi K^+\pi^-$ **(0.0325)**
$\overline{B^0}(\overline{d}b)$	**5.2794**	**460**	**10.5**	$D^+\pi^-$ **(0.276)**, $J/\psi K^-\pi^+$ **(0.0325)**
$B_c^+(c\overline{b})$	**6.4**			$J/\psi\pi^+$ **(0.0082)**
$B_c^-(\overline{c}b)$	**6.4**			$J/\psi\pi^-$ **(0.0082)**
$\Lambda_b^0(udb)$	**5.624**	**368**		$J/\psi\Lambda$ **(0.047)**, $\Lambda_c^+\pi^-$ **(seen)**

Table 1: Some charm and bottom hadrons with their mass, decay length (when given), branching ratios to leptons (when applicable) and some selected decays to hadrons.

p_T Asymmetry $A_T = |(p_{T_1} - p_{T_2})/(p_{T_1} + p_{T_2})|$

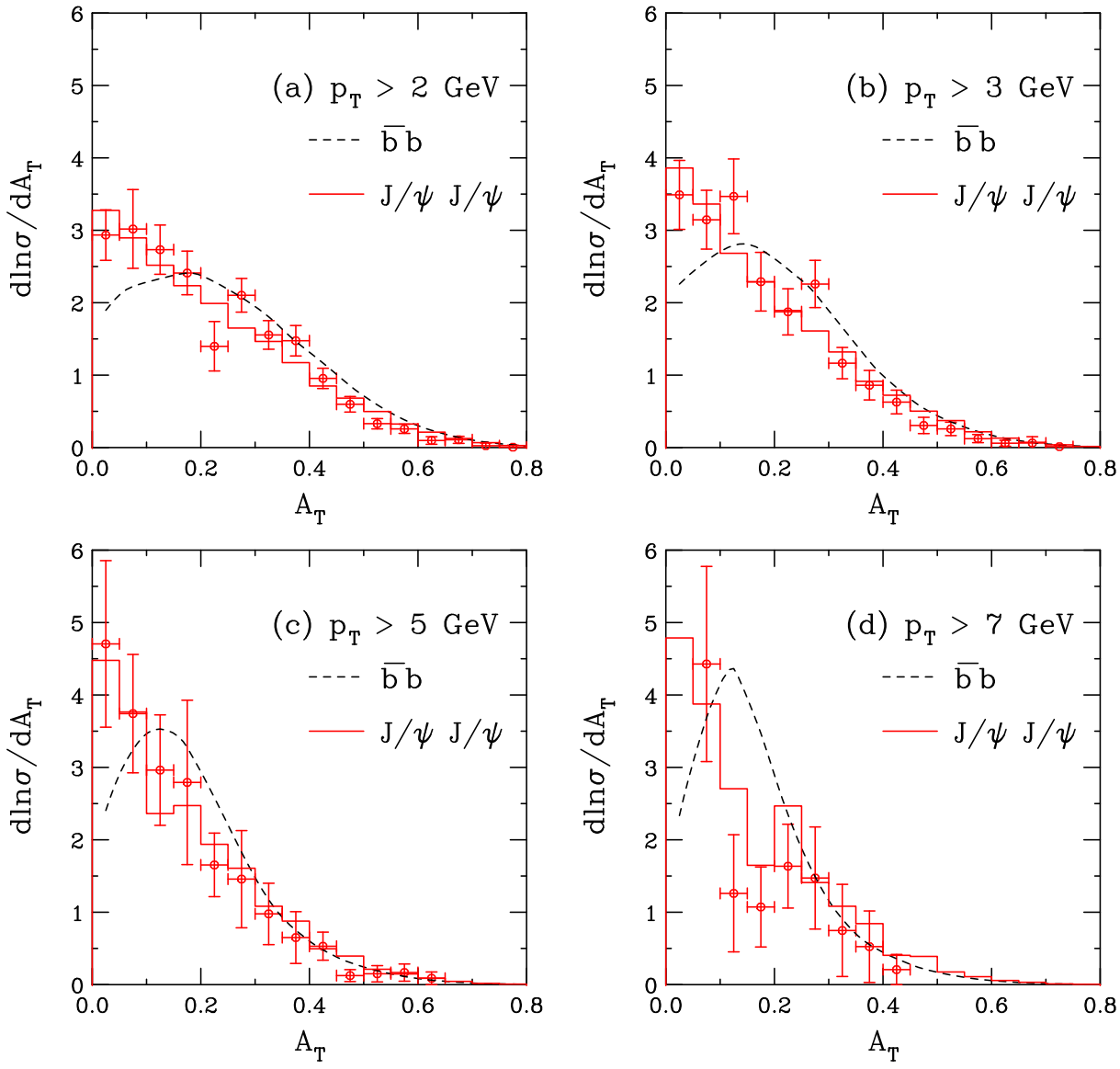

Figure 30: **The p_T asymmetry between the b and $\bar{b}$ (black dashed lines) and the J/ψ's resulting from B decays (red histograms) are compared to the LHCb data (red circles) for p_T cuts on the B and the J/ψ of 2 (a), 3 (b), 5 (c) and 7 GeV (d).**

Pair p_{T_p} Distributions

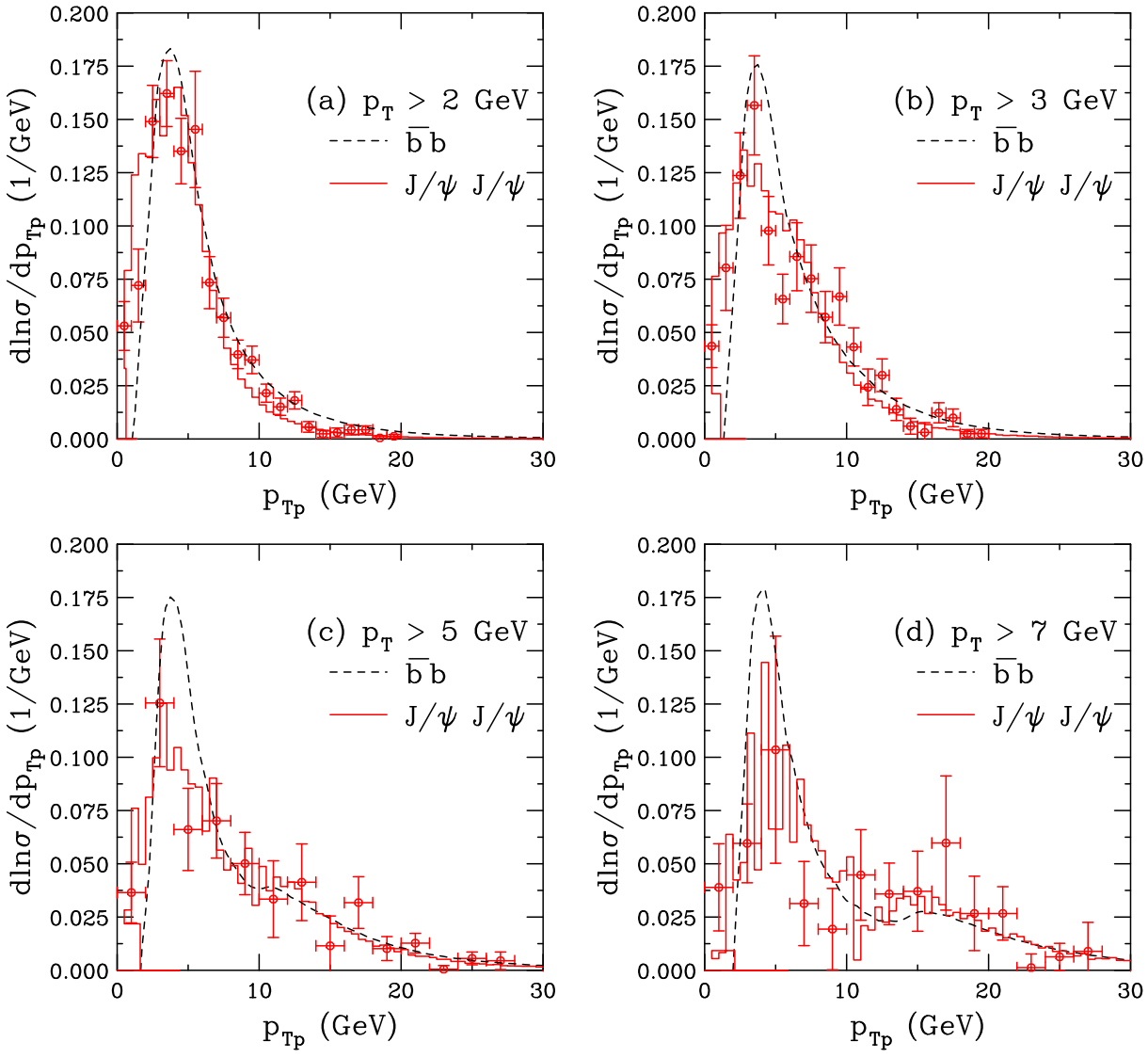

Figure 31: **The transverse momentum of the b and $\overline{b}$ (black dashed lines) and the J/ψ's resulting from B decays (red histograms) are shown compared to the LHCb data (red circles) for the p_T cuts on the B and the J/ψ of 2 (a), 3 (b), 5 (c) and 7 GeV (d).**

Sensitivity to $\langle k_T^2 \rangle$

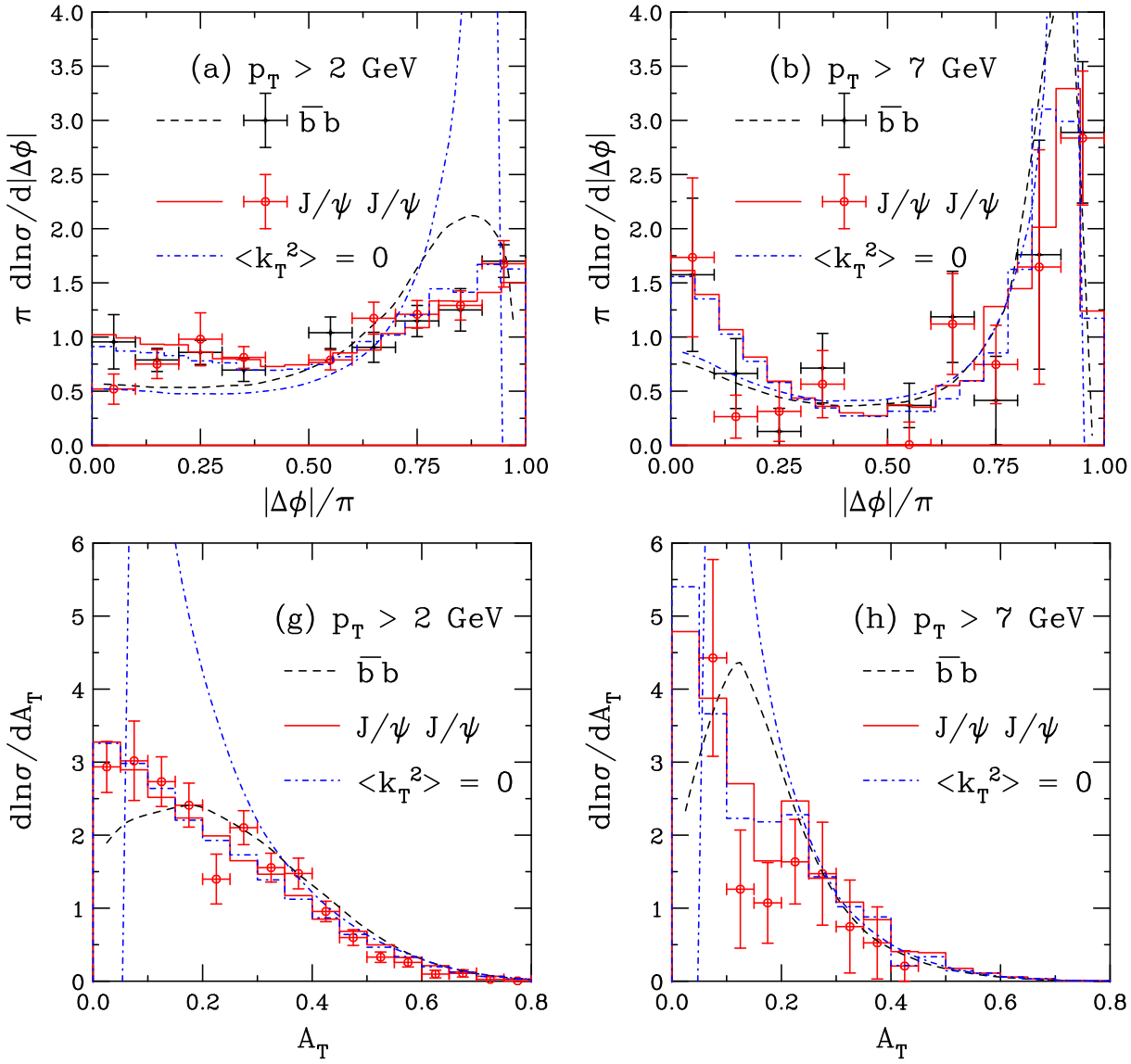

Figure 32: **The difference in the $b\bar{b}$ and $J/psiJ/\psi$ pair results for $\langle k_T^2 \rangle = 0$ and the default k_T kick. The $\langle k_T^2 \rangle = 0$ results are shown by the blue dot-dashed curves ($b\bar{b}$) and blue dot-dashed histograms ($J/\psi J/\psi$) and with the default k_T kick by the black dashed curves ($b\bar{b}$) and red histograms ($J/\psi J/\psi$). Results are shown for the azimuthal angle difference (a) and (b) and p_T asymmetry (g) and (h).**